Atmos. Chem. Phys. Discuss., 9, 2559–2608, 2009
www.atmos-chem-phys-discuss.net/9/2559/2009/

Atmospheric Chemistry and Physics Discussions

This discussion paper is/has been under review for the journal *Atmospheric Chemistry and Physics (ACP)*. Please refer to the corresponding final paper in *ACP* if available.

The radiative forcing potential of different climate geoengineering options

T. M. Lenton[1,2] **and N. E. Vaughan**[1,2]

[1]School of Environmental Sciences, University of East Anglia, Norwich NR4 7TJ, UK
[2]Tyndall Centre for Climate Change Research, UK

Received: 10 December 2008 – Accepted: 11 December 2008 – Published: 28 January 2009

Correspondence to: T. M. Lenton (t.lenton@uea.ac.uk)

Published by Copernicus Publications on behalf of the European Geosciences Union.

Abstract

Climate geoengineering proposals seek to rectify the Earth's current radiative imbalance, either by reducing the absorption of incoming solar (shortwave) radiation, or by removing CO_2 from the atmosphere and transferring it to long-lived reservoirs, thus increasing outgoing longwave radiation. A fundamental criterion for evaluating geoengineering options is their climate cooling effectiveness, which we quantify here in terms of radiative forcing potential. We use a simple analytical approach, based on the global energy balance and pulse response functions for the decay of CO_2 perturbations. This aids transparency compared to calculations with complex numerical models, but is not intended to be definitive. Already it reveals some significant errors in existing calculations, and it allows us to compare the relative effectiveness of a range of proposals. By 2050, only stratospheric aerosol injections or sunshades in space have the potential to cool the climate back toward its pre-industrial state, but some land carbon cycle geoengineering options are of comparable magnitude to mitigation "wedges". Strong mitigation, i.e. large reductions in CO_2 emissions, combined with global-scale air capture and storage, afforestation, and bio-char production, i.e. enhanced CO_2 sinks, might be able to bring CO_2 back to its pre-industrial level by 2100, thus removing the need for other geoengineering. Alternatively, strong mitigation stabilising CO_2 at 500 ppm, combined with geoengineered increases in the albedo of marine stratiform clouds, grasslands, croplands and human settlements might achieve a patchy cancellation of radiative forcing. Ocean fertilisation options are only worthwhile if sustained on a millennial timescale and phosphorus addition probably has greater long-term potential than iron or nitrogen fertilisation. Enhancing ocean upwelling or downwelling have trivial effects on any meaningful timescale. Our approach provides a common framework for the evaluation of climate geoengineering proposals, and our results should help inform the prioritisation of further research into them.

1 Introduction

Geoengineering has been defined as "large-scale engineering of our environment in order to combat or counteract the effects of changes in atmospheric chemistry" (NAS, 1992), in particular to mediate the effects of elevated greenhouse gas, especially carbon dioxide (CO_2), concentrations. In contrast, mitigation refers to activities that reduce anthropogenic emissions of greenhouse gases (particularly CO_2). The realisation that existing mitigation efforts are proving wholly ineffectual at the global scale, as evidenced by post-2000 trends in anthropogenic CO_2 emissions (Canadell et al., 2007), has fuelled a recent resurgence of interest in geoengineering (Crutzen, 2006), with a growing number of proposals being aired in the scientific literature (Boyd, 2008). The proposed roles for geoengineering vary from perpetually counteracting the radiative forcing due to mitigated anthropogenic greenhouse gas emissions (Wigley, 2006), to only being deployed if dangerous climate change is imminent or underway (Angel, 2006). Either way, accurate quantifications of potential climate cooling effects is crucial. Yet there is something of a shortage of these, especially for carbon cycle geoengineering proposals where most efforts stop at quantifying an effect on atmospheric CO_2 (if indeed they get that far). Also, the enthusiasm of proponents has led to some exaggerated claims of the effectiveness of some geoengineering proposals, as we will show. As part of a broader review of climate geoengineering proposals to be published separately (Vaughan and Lenton, 2009), we have sought to quantify, in a common currency, the climate cooling potential of a wide range of geoengineering proposals discussed in the recent literature. "Will it be effective?" is certainly not the only criterion against which geoengineering proposals should be judged (Boyd, 2008), but it serves as a "knock out" criterion: Only measures that pass the basic test of potential effectiveness need be considered further.

At the simplest level, the surface temperature of the Earth results from the net balance of incoming solar (shortwave) radiation and outgoing terrestrial (longwave) radiation (Kiehl and Trenberth, 1997). Geoengineering options (Fig. 1) attempt to rectify

the current radiative imbalance via either: (1) reducing the amount of solar (shortwave) radiation absorbed by the Earth, or (2) increasing the amount of longwave radiation emitted by the Earth. The shortwave options (1) can be subdivided into (a) those that seek to reduce the amount of solar radiation reaching the top of the atmosphere, and (b) those that seek to increase the reflection of shortwave radiation (albedo) within the atmosphere or at the surface. The longwave options (2) primarily involve removing CO_2 from the atmosphere and preventing (at least some of) it from returning there. They can be subdivided into the enhancement or creation of (a) land and (b) ocean carbon sinks. Other climate geoengineering approaches are conceivable, for example, increasing shortwave absorption in the stratosphere by injecting soot particles (Crutzen, 2006), or increasing outgoing longwave radiation by dispersing clouds over the polar ice caps, but we confine our attention to proposals focused on in the recent literature.

Shortwave geoengineering proposals (Fig. 1) start with reflecting away (or shading out, as seen from Earth) a fraction of incoming solar radiation by placing objects in a solar orbit, e.g. at the inner Lagrange point (L1) (Angel, 2006). Alternatively, sunshades could be placed in an Earth orbit (NAS, 1992; Pearson et al., 2006). Once solar radiation enters the atmosphere, its reflection back to space could be enhanced by adding sulphate aerosol (Crutzen, 2006) or manufactured particles (Teller et al., 1997, 2002) to the stratosphere. Adding such aerosols to the troposphere (NAS, 1992) has been ruled out due to negative impacts on human health, the greater loading required than the equivalent intervention in the stratosphere, and the need for multiple injection locations (Crutzen, 2006; MacCracken, 2006). However, increasing the reflectivity of low level marine stratiform clouds by mechanical (Latham, 1990) or biological (Wingenter et al., 2007) generation of cloud condensation nuclei (CCN) is being considered. Finally, the reflectivity of the Earth's surface could be increased, with recent proposals focused on the land surface, including albedo modification of deserts (Gaskill, 2004), grasslands (Hamwey, 2007), croplands (Ridgwell et al., 2009), human settlements (Hamwey, 2007), and urban areas (Akbari et al., 2008).

Options for enhancing the land carbon sink (Fig. 1), involve increasing the net uptake of CO_2 (either by plants or by chemical means) and successfully storing the captured carbon either in vegetation biomass, in soils, or in geological storage sites. Afforestation and reforestation sequesters carbon in the biomass of trees (NAS, 1992), and is also currently treated as a mitigation option by the Intergovernmental Panel on Climate Change (IPCC). The production of bio-char by pyrolysis (combustion largely in the absence of oxygen), converts roughly 50% of the carbon in biomass to a long-lived form – charcoal, which can then be added to soils (the rest produces CO_2 which can also be captured and stored) (Lehmann et al., 2006). Air capture and storage is used here to cover two recently favoured pathways of capturing CO_2 from the "free air" and conveying it to geological storage sites. Bio-energy with carbon storage (BECS) refers to a variety of biomass and bio-fuel production pathways, based around forestry, sugar cane and switchgrass production, followed by capture and storage of the CO_2 produced in the process of fermenting fuels and in combustion, followed by carbon storage (Read and Lermit, 2005). Chemical capture and storage is achieved by using ambient (wind) or actively-generated flow over a sorbent material (such as sodium hydroxide, NaOH) resulting in a pure stream of CO_2 gas which is then compressed and transported to a storage site (Zeman, 2007; Keith et al., 2006).

Options for enhancing the ocean carbon sink (Fig. 1) generally depend on successfully transporting more carbon to the deep ocean, via either the biological (soft tissue) pump or the solubility pump, and increasing carbon storage there. We also consider the potential for increasing carbon storage in coastal and shelf sea sediments via increased nutrient (especially phosphorus) runoff from the land. Suggestions for enhancing the biological (soft tissue) pump involve adding limiting nutrients derived from the land surface to appropriate surface areas of the ocean (Lampitt et al., 2008), including phosphorus, nitrogen and iron, or enhancing the upwelling of nutrient-rich waters (Lovelock and Rapley, 2007), potentially stimulating nitrogen fixation (Karl and Letelier, 2008). Suggestions for enhancing the solubility pump include increasing deep water production (i.e. downwelling in key regions) (Zhou and Flynn, 2005). Alternatively, in-

creasing the alkalinity of the oceans through the addition of carbonate minerals should allow more CO_2 to be absorbed (Kheshgi, 1995; Harvey, 2008).

To compare these geoengineering options, we quantify the potential of each to cool the climate, in terms of radiative forcing (RF), and compare our simple estimates to published values, where they exist. In broad terms, radiative forcing describes any imbalance in Earth's radiation budget caused by human interventions in the climate system. Once radiative forcing is applied, the climate system tends to adjust to recover energy balance, which usually takes the form of changes in temperature at various levels. The IPCC convention is to measure radiative forcing in terms of the change in net irradiance at the tropopause, after allowing stratospheric temperatures to readjust to radiative equilibrium (IPCC, 2001, 2007). The tropopause is chosen because there is a direct relationship between radiative forcing across it and surface temperature change; $\Delta T_s = \lambda\,\mathrm{RF}$, where λ is a climate sensitivity parameter. This relationship holds reasonably well (within a given model) for most forcing factors, especially changes in well mixed greenhouse gases. However, the true value of λ is poorly known, ranging over 0.6 to 1.2°C W^{-1} m^2 in current models, with a value of λ=0.86°C W^{-1} m^2 corresponding to their mean equilibrium response to doubling CO_2 of ΔT_s=3.2°C (IPCC, 2007). Allowing stratospheric temperatures to adjust is important for correctly evaluating the effect of changes in stratospheric ozone concentration and has a 5–10% effect on the forcing due to some other greenhouse gases, but it is less important for shortwave forcing agents. For most shortwave forcing agents, the instantaneous radiative forcing at the top of the atmosphere (TOA) is linked to surface temperature change and can be substituted for the stratospheric-adjusted radiative forcing at the tropopause (IPCC, 2007). We calculate the effect of different shortwave geoengineering options on the instantaneous TOA radiative forcing, because this allows us to make use of the shortwave part of the Earth's annual global mean energy budget (Kiehl and Trenberth, 1997). We compare the resulting values to the effect of different CO_2 geoengineering options on the stratospheric-adjusted radiative forcing at the tropopause, calculated from a well-known, simple formula (IPCC, 2001, 2007).

In the geoengineering literature, either the present anthropogenic radiative forcing ($+1.6\,[-1.0/+0.8]\,W\,m^{-2}$ in 2005) or that due to a doubling of atmospheric CO_2 ($+3.71\,W\,m^{-2}$) (IPCC, 2007), are typically taken as the targets to counteract. However, actual anthropogenic radiative forcing has varied, and will continue to vary, over time. By radiative forcing "potential" we generally mean the most negative radiative forcing that could physically be achieved by a particular option (irrespective of whether it is sensible or desirable, for other reasons, to achieve it). The exceptions are space-based measures which have considerable capacity to be scaled up and atmospheric aerosol and CCN measures which have limited capacity to be scaled up. Geoengineered radiative forcing effects themselves will all decay over time, although at widely differing rates. Shortwave geoengineering options generally have rather short lifetimes (from a few decades for spacecraft at the L1 point, a few years for stratospheric sulphate, to a few hours for tropospheric CCN). This is usually addressed by arguing that short-lived measures would be continually replenished, and we calculate their radiative forcing potential on this basis, making them appear time-independent. In truth, all the options would take some time to develop and deploy and may never reach their estimated potential.

The longwave geoengineering options have to be considered in a time dependent manner, because they involve interfering with a dynamic carbon cycle. Hence we consider time-dependent scenarios of CO_2 removal from the atmosphere. There is an added complication that effects on atmospheric CO_2 will decay over time, due to the counter-balancing response of ocean and land carbon reservoirs to atmospheric perturbations. Effects will also decay if carbon storage is not permanent and CO_2 is leaked back to the atmosphere. Thus, to calculate an effect on atmospheric CO_2 one must specify a timescale of interest. To calculate a corresponding impact on radiative forcing one also needs to account for the fact that the sensitivity of radiative forcing to a given change in CO_2 depends inversely on the absolute concentration of CO_2 (see Sect. 2.2). This demands that we specify a reference scenario for CO_2 concentration. We choose to focus on two intermediate time horizons of interest to policy makers,

2050 and 2100, and also consider long-term effects on the millennial timescale. Ultimately, the only way to return atmospheric CO_2 to pre-industrial levels is to permanently store (in some combination of the crust, sediments, soils, ocean, and terrestrial biosphere) an equivalent amount of CO_2 to the total emitted to the atmosphere.

We deliberately take a simple analytical approach to quantify radiative forcing potentials, based on the global energy balance and pulse response functions for the decay of CO_2 perturbations. The aim is to provide transparent results that are accurate to first order, in contrast to calculations with complex numerical models where one can never see exactly how the results are derived. The direct comparison of somewhat different shortwave and longwave radiative forcing measures appears reasonable in this context. Our approach is at a similar (or somewhat higher) level of complexity to analytical calculations in the geoengineering literature, with some notable exceptions, e.g. Hamwey (2007). Despite its simplicity, our approach reveals a number of significant errors in existing calculations in the literature, and it allows us to compare the relative effectiveness of a range of proposals. It is not intended to be definitive. Clearly our estimates can be improved upon and we encourage interested readers to do so.

2 Methods

2.1 Shortwave options

We quantify shortwave geoengineering options based on simple considerations of their instantaneous effect on the Earth's annual global mean energy balance at the top of the atmosphere (TOA) (Kiehl and Trenberth, 1997). The annual global mean flux of solar radiation at the TOA is S_0=342 $W\,m^{-2}$, 77 $W\,m^{-2}$ of this is reflected in the atmosphere by clouds and aerosols and 67 $W\,m^{-2}$ is absorbed in the atmosphere, leaving 198 $W\,m^{-2}$ to reach the surface, where 30 $W\,m^{-2}$ is reflected and 168 $W\,m^{-2}$ is absorbed. In total, 107 $W\,m^{-2}$ is reflected back to space corresponding to an average planetary albedo, α_p=107/342=0.313, and a total absorption of 265 $W\,m^{-2}$. Short-

wave geoengineering proposals aim to decrease the 265 W m^{-2} absorbed, either by shading the Earth, or by increasing the planetary albedo.

For measures that seek to reduce the amount of solar radiation reaching the Earth, by ΔS (W m^{-2}), the resulting instantaneous TOA radiative forcing, RF is given by:

$$\mathrm{RF} = \Delta S(1 - \alpha_p) \quad (1)$$

In other words, the reduction in incoming solar radiation must exceed the required radiative forcing by a factor of $1/(1-\alpha_p)$=1.456.

For measures that seek to increase the planetary albedo by an amount $\Delta\alpha_p$, the corresponding instantaneous TOA radiative forcing is given by:

$$\mathrm{RF} = -S_0\Delta\alpha_p \quad (2)$$

However, changes in atmosphere/cloud or surface albedo, even if globally and uniformly applied, do not produce equivalent changes in planetary albedo. To estimate their effect on the planetary albedo with reasonable accuracy requires a simple model of the shortwave energy balance.

We make the approximation that there are two reflective layers that contribute to the planetary albedo, one at the surface with albedo α_s, and one in the atmosphere with albedo α_a. Atmospheric shortwave absorption is assumed to occur in a discrete layer with absorption fraction, A_a, defined as the fraction of the shortwave flux reaching this layer that is absorbed. Multiple reflections and absorptions are neglected. In practice, the altitude of a change in atmospheric albedo will determine how much absorption has occurred before reflection, which in turn will alter the impact of a given atmospheric albedo change on the planetary albedo. We consider the two limiting cases; all reflection before all absorption, and all absorption before all reflection. Surface albedo, α_s=30/168=0.152, is the same regardless of the order in which atmospheric reflection and absorption occur.

First consider the case of a reflective layer at the top of the atmosphere (TOA) beneath which all atmospheric absorption occurs. This is a reasonable approximation for

proposals to increase stratospheric reflection. In this case, planetary albedo is related to atmosphere and surface albedos by:

$$\alpha_p = \alpha_a + \alpha_s(1 - \alpha_a)(1 - A_a) \quad (3)$$

with atmospheric albedo α_a=77/342=0.225 and atmospheric absorption A_a=67/265=0.253 consistent with the current global energy balance (Kiehl and Trenberth, 1997). Even though reflection occurs at the top of the atmosphere, changes in atmospheric albedo produce proportionately smaller changes in planetary albedo, because there is a counteracting change in reflection from the surface:

$$\Delta\alpha_p = \Delta\alpha_a(1 - \alpha_s(1 - A_a)) = 0.886\Delta\alpha_a \quad (4)$$

Alternatively, consider the case of a reflective layer just above the surface, above which all atmospheric absorption occurs. This is a reasonable approximation for proposals to increase reflection from low-level marine stratiform clouds. In this case, planetary albedo is related to atmosphere and surface albedo by:

$$\alpha_p = \alpha_a(1 - A_a) + \alpha_s(1 - \alpha_a)(1 - A_a) \quad (5)$$

with atmospheric absorption A_a=67/342=0.196 and atmospheric albedo α_a=77/275=0.280 consistent with the current global energy balance (Kiehl and Trenberth, 1997). The effect of changes in (low-level) atmospheric albedo on planetary albedo is reduced relative to Eq. (4) because the shortwave flux reaching the reflective layer is reduced by prior absorption:

$$\Delta\alpha_p = \Delta\alpha_a(1 - \alpha_s)(1 - A_a) = 0.682\Delta\alpha_a \quad (6)$$

In both cases, changes in surface albedo have the same effect on the planetary albedo, producing even smaller changes:

$$\Delta\alpha_p = \Delta\alpha_s(1 - \alpha_a)(1 - A_a) = 0.579\Delta\alpha_s \quad (7)$$

This is because the flux of radiation reaching the surface is only 198/342=0.579 of the flux at the top of the atmosphere. (The same result is obtained for the different

combinations of A_a and α_a because the shortwave flux reaching the surface is the same).

For geoengineering proposals where the albedo change covers only a fraction of the Earth's surface area, we multiply the quoted change in albedo by the fraction of the Earth's surface area affected, f_{Earth}. Data for areal coverage of different land surface types were obtained from the International Geosphere-Biosphere Programme – Data and Information System (IGBP-DIS) (Loveland et al., 2000) and/or University of Maryland (UMd) (Hansen et al., 2000) land cover datasets. The resulting albedo change is then inserted into the appropriate choice of Eqs. (4), (6) or (7) and the result of that inserted into Eq. (2).

2.2 Longwave (CO_2) options

We quantify longwave geoengineering options based on their effect on atmospheric CO_2 concentration and hence the stratospheric-adjusted radiative forcing at the tropopause (IPCC, 2001, 2007). The radiative forcing due to specific carbon cycle geoengineering activities depends both on their effect on atmospheric CO_2 at a given time and on the absolute value of atmospheric CO_2 at that time. Radiative forcing is, to a reasonable approximation, a logarithmic function of CO_2:

$$\text{RF} = \beta \ln \frac{C}{C_{\text{ref}}} \tag{8}$$

Here C is the concentration of atmospheric CO_2 after a given time, C_{ref} is a reference concentration, and $\beta = 5.35\,\text{W m}^{-2}$ from (IPCC, 2001). Typically the pre-industrial $C_{1800} = 278\,\text{ppm} = C_{\text{ref}}$ is specified. Then, for example, the 2005 value of $C = 379\,\text{ppm}$ resulted in an RF of $1.66\,\text{W m}^{-2}$ (IPCC, 2007). The logarithmic relationship means that the sensitivity of RF to CO_2 ($\text{W m}^{-2}\,\text{ppm}^{-1}$) is inversely related to the concentration of CO_2:

$$\frac{\text{dRF}}{\text{d}C} = \frac{\beta}{C} \tag{9}$$

Thus the present sensitivity (using a 2005 concentration of $C = 379\,\text{ppm}$) is $0.0141\,\text{W m}^{-2}\,\text{ppm}^{-1}$, whereas the pre-industrial sensitivity was $0.0192\,\text{W m}^{-2}\,\text{ppm}^{-1}$ and at double pre-industrial CO_2 the sensitivity will be $0.0096\,\text{W m}^{-2}\,\text{ppm}^{-1}$. In general, the radiative forcing effect of a particular carbon cycle geoengineering activity at a given time, t, can be calculated from:

$$\text{RF}(t) \approx \frac{\Delta C_{\text{atm}}}{k} \frac{\beta}{C(t)} \tag{10}$$

where ΔC_{atm} (in PgC) is the amount of CO_2 that has been removed from the atmosphere at that time (hence a negative number), $k = 2.14\,\text{PgC ppm}^{-1}$ is a simple conversion factor, and $C(t)$ is the reference state that atmospheric CO_2 would be in, in the absence of geoengineering, at that time. This immediately suggests a potential synergy between mitigation action (reducing C) and the effectiveness of carbon cycle geoengineering (increasing the magnitude of ΔC_{atm}) because a given reduction in atmospheric CO_2 has a greater radiative forcing effect at lower CO_2. However, as we will show below, a given geoengineering scenario ultimately has a greater effect on CO_2 at higher concentrations of CO_2 (i.e. in scenarios with larger total emissions). To make estimates of RF(t) we calculate ΔC_{atm} and specify a reference $C(t)$.

First we consider the calculation of effects on atmospheric CO_2 (ΔC_{atm}) over time. Adding CO_2 to the atmosphere or removing CO_2 from the atmosphere triggers responses from the ocean and land reservoirs that are continuously exchanging CO_2 with the atmosphere. The result is that any perturbation to atmospheric CO_2, whether an increase or a decrease, decays over time towards around 20% of its original size on a millennial timescale. The fraction of the original perturbation remaining after a given time, Δt (in years), is called the airborne fraction, $f(\Delta t)$. It is a complex function containing multiple decay timescales, related to multiple land and ocean carbon reservoirs. For relatively small perturbations, it can be approximated, from the Bern carbon cycle model (Joos et al., 1996) by:

$$f(\Delta t) = 0.18 + 0.14e^{-\Delta t/420} + 0.18e^{-\Delta t/70} + 0.24e^{-\Delta t/21} + 0.26e^{-\Delta t/3.4} \tag{11}$$

According to this formula, for an instantaneous removal of carbon from (or release to) the atmosphere, 92% is still removed (or present) after 1 year, 64% after 10 years, 34% after 100 years, and 19% after 1000 years. This is a little confusing when compared with observations over 1960–2007 that the increase in atmospheric CO_2 in a given year was only ~50% of the total emissions that year. The discrepancy can be explained by the fact that in any given year, the natural land and ocean carbon sinks represent an integrated response to all previous years of emissions.

For completeness we note that the amount of carbon sequestered by a particular geoengineering activity can also decay over time, if the reservoir to which the carbon is added is not permanently isolated from the atmosphere. To account for this we can introduce the notion of a stored fraction, $g(\Delta t)$. Clearly for some sequestration options there will be multiple decay timescales, as there are for the atmosphere in Eq. (11). As a first approximation we can assume exponential decay of storage, with an e-folding timescale, τ:

$$g(\Delta t) = e^{-\Delta t/\tau} \tag{12}$$

Now consider a specific carbon cycle geoengineering scenario, $R(t)$, which starts in year t_s and involves the removal of CO_2 from the atmosphere as some function of time until it stops in year t_c (here the removal flux is defined as positive). The amount of CO_2 which has been removed from the atmosphere, ΔC_{atm}, at some future time, t_f, can be found by integrating (over the interval t_s to t_c) the product of the removal function, its remaining stored fraction, and the remaining airborne fraction of that:

$$\Delta C_{\text{atm}} = -\int_{t_s}^{t_c} R(t)g(t_f - t)f(t_f - t)dt \tag{13}$$

We solve this integral using Eqs. (11) and (12) and three simple cases for $R(t)$ that have been presented in the literature: (a) constant removal, $R=a$, (b) linearly increasing removal with time, $R(t)=b(t-t_s)$, and (c) exponentially increasing removal with time, $R(t)=E_0e^{c(t-ts)}$ (see Appendix A). In general, we assume that the earliest time that a

particular carbon cycle geoengineering activity could start is t_s=2020, although exceptions are made for some scenarios in the literature that start earlier. Unfortunately, information on the value of τ is lacking for some reservoirs, or they have multiple decay timescales. As we are seeking to quantify the maximum potential of each option, in the results presented we assume permanent sequestration, i.e. $g(\Delta t)$=1, thus simplifying the integrals (see Appendix A). For relatively short-lived storage reservoirs such as vegetation biomass this amounts to assuming that they will be continually replenished as they decay. For the most complex case of measures to increase deep ocean carbon storage we estimate the "sequestration flux" of carbon that crosses the depth of winter mixing and assume it is permanently stored on the timescales considered, whereas any additional carbon that is remineralised above this depth is assumed to be instantaneously returned to the atmosphere.

Now we turn to the choice of the reference trajectory of atmospheric CO_2, $C(t)$. Clearly this will be a complex function of time, determined by emissions and natural sinks. To minimise errors introduced by non-linear feedbacks in the carbon cycle (and for consistency with the formulation of Eq. 11 for relatively small perturbations), we consider as a baseline a strong mitigation scenario with minimum reference CO_2 concentration at key times in the future. We pick out two medium-term time horizons, 2050 and 2100, of particular interest to policy makers. In 2050, with strong mitigation, CO_2 could be restricted to about 450 ppm (Kharecha and Hansen, 2008) (although even linearly extrapolating the current concentration growth rate of 2 ppm yr^{-1} it will be close to 470 ppm). In 2100, with strong mitigation (but without geoengineered "negative emissions"), CO_2 could be restricted to about 500 ppm. Most studies considering a lower stabilisation target of 450 ppm, e.g. (Stern, 2006), have to invoke negative emissions to achieve it, with a recent exception (Kharecha and Hansen, 2008). For reference, without mitigation and with strong positive carbon cycle-climate feedbacks, CO_2 could reach about 600 ppm in 2050, rising to about 1000 ppm in 2100 (Cox et al., 2000; Lenton, 2000; Friedlingstein et al., 2006).

Over long (millennial) timescales, long after a given geoengineering activity has ceased, the increase in atmospheric CO_2 will depend on cumulative emissions, ΣC_{emit}, minus the amount of carbon "permanently" sequestered by a given geoengineering option on this timescale, ΣC_{seq}, times the long term airborne fraction (i.e. the first term in Eq. 11), which we now call f_{final}. The radiative forcing effect of the geoengineering option can then be calculated from Eq. (8) by taking C_{ref} to be the expected CO_2 in the absence of geoengineering and C to be the actual CO_2, which gives:

$$\text{RF}_{\text{final}} \approx \beta \ln \left(\frac{C_{1800} + f_{\text{final}} \left(\Sigma C_{\text{emit}} - \Sigma C_{\text{seq}} \right) / k}{C_{1800} + f_{\text{final}} \Sigma C_{\text{emit}} / k} \right) \tag{14}$$

According to Eq. (11), the airborne fraction shrinks towards $f_{\text{final}}=0.18$, and is 0.193 after 1000 years (i.e. around year 3000). However, an important caveat is that f_{final} actually increases with the net amount of CO_2 added to the ocean-atmosphere-land system, as a consequence of ocean carbonate chemistry and positive climate-carbon cycle feedbacks (Lenton, 2006). To get an estimate of how f_{final} varies as a function of net carbon addition we find a good fit to numerical model results (Lenton, 2006) (<1.5% error for 0–5000 PgC), is given by:

$$f_{\text{final}}=0.152e^{0.000179\ \Sigma C_{\text{added}}} \tag{15}$$

where $\Sigma C_{\text{added}}=\Sigma C_{\text{emit}}$ in the reference case and $\Sigma C_{\text{added}}=\Sigma C_{\text{emit}}-\Sigma C_{\text{seq}}$ in the geoengineering case. In this numerical model (Lenton, 2006) the minimum airborne fraction is smaller than in Eq. (11) (Joos et al., 1996). However, even with strong mitigation, a realistic lower limit on cumulative emissions is $\Sigma C_{\text{emit}}=1000$ PgC, which is roughly twice the emissions to date. Since 1800, around 350 PgC has been emitted from fossil fuel burning, and up to 165 PgC from land-use change emissions. This gives $f_{\text{final}}=0.18$ consistent with our earlier assumptions.

Using Eq. (15) in (14), we find an interesting result; that although a given change in atmospheric CO_2 has a greater impact on radiative forcing at lower concentrations of CO_2 a given sequestration of carbon has a greater impact on atmospheric

CO_2 if total emissions of carbon are greater. The two effects approximately cancel such that a given permanent sequestration of carbon has roughly the same impact on radiative forcing regardless of the total emissions of carbon. To illustrate this, consider a no-mitigation scenario, where all conventional fossil fuel resources are assumed to be combusted between 1800 and 3000, giving cumulative CO_2 emissions of order $\Sigma C_{\text{emit}}=5000$ PgC (2336 ppm). The corresponding $f_{\text{final}}=0.372$, gives a reference 1147 ppm in the atmosphere (roughly 4 times the pre-industrial level) and a corresponding radiative forcing of 7.58 W m^{-2}. In contrast, in our strong mitigation scenario, with $\Sigma C_{\text{emit}}=1000$ PgC (467 ppm) and $f_{\text{final}}=0.182$, the final atmospheric concentration is 363 ppm with a corresponding radiative forcing of 1.43 W m^{-2}. For 100 PgC permanently sequestered, in the strong mitigation case CO_2 is lowered by 10 ppm, whereas in the no mitigation case CO_2 is lowered by 32 ppm, but in both cases, $\text{RF}_{\text{final}}\approx-0.15$ W m^{-2}. For 1000 PgC permanently sequestered, in the strong mitigation case $\text{RF}_{\text{final}}\approx-1.43$ W m^{-2} (returning CO_2 to 278 ppm and completely cancelling the radiative forcing that would have occurred due to 1000 PgC emissions), whereas in the no mitigation case $\text{RF}_{\text{final}}\approx-1.54$ W m^{-2} (due to lowering CO_2 from 1147 ppm to 859 ppm).

In the following, we offer upper estimates of the potential of different carbon cycle geoengineering options, concentrating on the time horizons of 2050, 2100 and 3000. To calculate intermediate timescale effects of particular geoengineering scenarios on atmospheric CO_2, we use solutions to Eq. (13) (see Appendix A), and convert this to radiative forcing using Eq. (10) and lower limits on atmospheric CO_2 at the time, consistent with strong mitigation. To estimate the long-term effects of different cumulative geoengineering activities, there are two options. For measures where reservoirs would not be saturated and activity is assumed to continue on the millennial timescale we use Eq. (13) with $t_c=t_f=3000$, and Eq. (10) assuming $C_{\text{ref}}=363$ ppm, i.e. strong mitigation. For measures where sequestration reservoirs could be filled well before 3000, we use Eqs. (14) and (15), together with estimates of their maximum potential long-term carbon storage, and total emissions corresponding to strong mitigation (1000 PgC). We

have also made calculations for a "no mitigation" (5000 PgC) scenario but the long-term radiative forcing effects generally do not differ significantly. To calculate the intermediate timescale effects of a "no mitigation" scenario one should ideally take into account the fact that the airborne fraction increases significantly with increasing emissions (i.e. the terms in Eq. 11 change). Preliminary estimates and Eq. (10) suggest that the resulting radiative forcing effects will be similar to or less than we obtain assuming a strong mitigation scenario.

3 Results

The results are summarised in Table 1 for shortwave options and Table 2 for longwave (CO_2) options.

3.1 Shortwave options

3.1.1 Sunshades in space

To offset a doubled pre-industrial atmospheric concentration of CO_2 is usually assumed to require a decrease in incoming solar radiation of roughly 1.8%, (e.g. Govindasamy and Caldeira, 2000), which using Eq. (1) gives a radiative forcing of RF=$-4.23\,W\,m^{-2}$. However, RF=$3.71\,W\,m^{-2}$ from doubling CO_2 is more accurate (IPCC, 2001, 2007) and the counteracting decrease in incoming solar radiation should be 1.58% (ΔS=$5.40\,W\,m^{-2}$). If such a reduction in incoming solar radiation were achieved by placing a sunshade consisting of multiple "flyers" at the L1 point (Angel, 2006), it would require a total area of 4.1 million km^2 (revised from 4.7 million km^2). The negative radiative forcing effect could be varied by altering the size of the sunshade. The calculations presented in the literature are based on a static radiative imbalance, however with the observed trends in emissions to date (Raupach et al., 2007) it is clear that the radiative imbalance is set to continue increasing. For example, if a sunshade

was in place today at the L1 point to offset the current radiative imbalance, then given that atmospheric CO_2 is rising at $2\,ppm\,yr^{-1}$ and converting this to $0.0282\,W\,m^{-2}\,yr^{-1}$ using Eq. (9), a surface area of $\sim$31 000 km^2 would need to be added each year. This equates to $\sim$135 000 launches per year, each carrying 800 000 space flyers of area $0.288\,m^2$ (Angel, 2006). Thus, the area of shades or reflectors in space would need to increase significantly year on year to keep pace with the current rate of increase in radiative forcing.

3.1.2 Stratospheric aerosols

To counteract the radiative forcing due to a doubling of atmospheric CO_2 ($3.71\,W\,m^{-2}$) by increasing the stratospheric reflection of shortwave radiation back to space (assuming no absorption occurs above the stratosphere), requires an average global increase in atmospheric albedo of $\Delta\alpha_a$=0.012 (Table 1). If this is achieved with sulphate aerosol, the amount required depends on the size of the particles and the location of injection, ranging from an estimated $1.5\,TgS\,yr^{-1}$ (Rasch et al., 2008) to $5\,TgS\,yr^{-1}$ (Crutzen, 2006; Wigley, 2006). Smaller particles (radius $\sim$0.1μm) are more effective because they have no impact in the longwave, while the larger, volcanic-like particles absorb and emit in the longwave (Stenchikov et al., 1998). The residence time and spatial spread of particles in the stratosphere varies greatly with the location of injection (Crutzen, 2006; Wigley, 2006; Rasch et al., 2008). Residence time and global coverage is maximised when injections occur into the lower stratosphere over the tropics (Oman et al., 2005; Robock et al., 2008). If manufactured particles are used instead of sulphate aerosol, the required mass loading could potentially be reduced by orders of magnitude (Teller et al., 1997, 2002).

3.1.3 Increase cloud albedo – mechanical

Marine stratiform cloud albedo could be globally increased by the mechanical generation of sea salt spray as a source of cloud condensation nuclei (CCN) (Latham, 1990).

It has been argued that a 50–100% increase in droplet concentration in all marine stratiform clouds would give rise to an increase in top-of-cloud albedo of 0.02, causing a planetary albedo increase of 0.005, and that this would offset a doubling of atmospheric CO_2 (Latham, 2002; Bower et al., 2006). However, an increase in planetary albedo of 0.005 gives a TOA radiative forcing of $-1.71\,W\,m^{-2}$ from Eq. (2), sufficient to offset the present anthropogenic radiative forcing, but not that from a doubling of CO_2, as noted in the original source (Charlson et al., 1987). To offset $3.71\,W\,m^{-2}$ from doubling CO_2 requires a planetary albedo increase of 0.011 (Latham et al., 2008). Furthermore, the original conversion from changes in top-of-cloud albedo to planetary albedo assumed 30% global coverage of marine stratiform clouds (i.e. 42% coverage over the ocean) and $\Delta\alpha_p = 0.83\,\Delta\alpha_a$ i.e. very little absorption before reflection – compare to Eqs. (4) and (6). Recently the numbers have been revised, considering non-overlapped marine stratiform clouds to cover 17.5% of the Earth's surface, a required change in top-of-cloud albedo of 0.062 is estimated (Latham et al., 2008). However, the revised calculation assumes that the change in low-level cloud albedo causes an identical change in planetary albedo, which would be wrong even if the clouds were at the top of the atmosphere. Instead they are near the surface and the change in planetary albedo could be less than 70% of the change in top-of-cloud albedo, from Eq. (6). Accounting for this, we estimate a required increase in top-of-cloud albedo of 0.091 (Table 1) across all regions of marine stratiform clouds. This is a markedly larger value than the often cited 0.02, but not inconceivable given that such clouds can range in albedo from 0.3 to 0.7. The CCN source required to achieve this change in albedo needs re-quantifying.

3.1.4 Increase cloud albedo – biological

An alternative proposal to enhance marine stratiform cloud albedo is to increase the biological source of CCN from dimethyl sulphide (DMS) emissions (Charlson et al., 1987) by iron fertilising a large patch of the Southern Ocean for one month in summer (Wingenter et al., 2007). It has been estimated that this could generate a 10% increase

in total CCN over the entire Southern Ocean (~10% of the Earth's surface) and a corresponding increase in cloud albedo by 0.008 (Wingenter et al., 2007). This was argued to be capable of causing a regional, seasonal radiative forcing of $\sim 3\,W\,m^{-2}$ (Wingenter et al., 2007), but this wrongly assumes the change in low-level cloud albedo causes an identical change in planetary albedo. Correcting for this and scaling by fraction of the year as well as fraction of the Earth's surface affected gives $\Delta\alpha_a = 0.000067$, and an annual global mean $RF = -0.016\,W\,m^{-2}$ (Table 1). This does not factor in that the TOA solar radiation over the Southern Ocean in summer is slightly more than the global annual average. Yet it is probably a significant overestimate as the increase in CCN over the Southern Ocean has subsequently been revised downwards to 2.6% (Vogt et al., 2008) or 1.4% (Woodhouse et al., 2008) giving a corresponding cloud albedo increase of ~0.002 or ~0.001 and a factor of 4 to 8 reduction in radiative forcing.

3.1.5 Increase desert albedo

It has been suggested at a meeting at the US Department of Energy (Gaskill, 2004) that increasing the albedo of global desert areas (up to $1.16\times10^{13}\,m^2$ deemed suitable) could counteract a significant amount of radiative forcing. These land areas are suggested because they are largely uninhabited, sparsely vegetated, flat and stable (aeolian deserts are excluded). Such deserts typically have an albedo in the range 0.2 to 0.5, depending on geologic composition (Tsvetsinskaya et al., 2002). An albedo increase from 0.36 to 0.8 has been proposed (Gaskill, 2004), with the addition of a reflective surface, made of white polyethylene top surface and an aluminium bottom surface. The application of this to 2% of Earth's surface ($1.0\times10^{13}\,m^2$) has been estimated to give $-2.75\,W\,m^{-2}$ radiative forcing (Gaskill, 2004), but from the global annual mean energy budget we get $RF = -1.74\,W\,m^{-2}$ (Table 1). The discrepancy may be because deserts generally have higher incident solar radiation than the global average value. The cooling effect of this option would clearly be biased to the regions altered.

3.1.6 Increase grassland albedo

Variegated plants, light shrubs or bioengineered grasses and shrubs could be used to increase the albedo of grassland, open shrubland and savannah globally by an estimated 0.0425 (25%) from 0.17 (Hamwey, 2007). Using a static 2-D radiative transfer model a predicted increase in global annual average surface albedo of $\Delta\alpha_s$=0.0026 and RF=−0.56 W m^{-2} are predicted (Hamwey, 2007). We use the total area of grassland, open shrubland and savannah from the IGBP-DIS land cover dataset (Loveland et al., 2000), and our cruder method to estimate $\Delta\alpha_s$=0.0032 and RF=−0.64 W m^{-2} (Table 1).

3.1.7 Increase cropland albedo

A similar proposal addresses croplands and assumes a default increase in maximum canopy albedo by 0.04 (20%) from 0.2 (Ridgwell et al., 2009). The area of croplands is considerably greater in the IGBP-DIS (Loveland et al., 2000) than the UMd (Hansen et al., 2000) land cover dataset (1.4×10^{13} m^2 versus 1.11×10^{13} m^2) giving a corresponding range in RF=−0.17 to −0.22 W m^{-2}. However, a 0.08 increase in maximum canopy albedo is argued to be feasible (Ridgwell et al., 2009), and we take this as an upper limit, which together with the upper area estimate gives RF=−0.44 W m^{-2} (Table 1). This proposal has been assessed in a coupled atmosphere-ocean model (HadCM3) with a dynamic global vegetation model (TRIFFID), designating areas of cropland in which only C_3 or C_4 grasses are allowed to grow, but not explicitly representing cropping (Ridgwell et al., 2009). For a change in maximum canopy albedo of 0.08, a global mean surface temperature change of −0.213±0.083°C is predicted relative to a control run with 700 ppm CO_2. Given a climate sensitivity parameter for this model of λ=0.89°C W^{-1} m^2 (IPCC, 2007) this suggests a radiative forcing of RF=−0.24± 0.09 W m^{-2} was generated in this model experiment, considerably less than our estimate. This may be explained by the actual canopy albedo change being less than the maximum 0.08 and/or a smaller area being covered by crops in the model.

3.1.8 Increase human settlement albedo

Albedo enhancement measures could potentially be applied to all areas of human settlement (Hamwey, 2007). A per capita value of 500 m^2 of human settlement has been assumed (Hamwey, 2007), and using 2005 global population data this gives a settled area of 0.64% of the Earth's surface (or 2.3% of the land surface). This area is assumed to have an albedo of 0.15, appropriate for the composite surface albedo of urban regions (Taha, 2008; Jin et al., 2005), and it is assumed it can be doubled to 0.3 (Hamwey, 2007). This albedo is apportioned over a 2-D radiative transfer model space to obtain a change in global surface albedo of $\Delta\alpha_s$=0.000875 and RF=−0.17 W m^{-2} (Hamwey, 2007). Using the same area and our cruder global approach, we obtain $\Delta\alpha_s$=0.00096 and RF=−0.19 W m^{-2} (Table 1).

3.1.9 Increase urban albedo

The albedo of urban regions can be increased by using highly reflective roofs and altering the material used in paving roads (Rosenfeld et al., 1997; Akbari et al., 2008). A proposed increase in the albedo of all urban roofs and pavements by 0.1 has been estimated to induce a radiative forcing of −0.044 W m^{-2}, based on 1% of the land surface being urban and 25% of this being roof area and 35% paved surface (i.e. 0.174% of the Earth's surface) (Akbari et al., 2008). Using the same $\Delta\alpha_s$=0.000174 we estimate RF=−0.034 W m^{-2}. However, the actual global urban area is far less than assumed (Akbari et al., 2008) at 2.6×10^{11} m^2 (Loveland et al., 2000; Hansen et al., 2000) or 0.051% of the Earth's surface, which gives RF=−0.01 W m^{-2} (Table 1).

3.2 Longwave (CO_2) options

3.2.1 Afforestation and reforestation

The most optimistic estimates suggest that 120 PgC could be accumulated by afforestation and reforestation by 2035 (Read, 2008; Read and Parshotam, 2007), assuming a linear increase in removal (at b=0.4 PgC yr^{-2}) from 0 PgC yr^{-1} in 2010 to 9.6 PgC yr^{-1} in 2034, i.e. around four times the current land carbon sink. This is followed by the accumulation a further 63 PgC in standing plantations by 2060 (i.e. 183 PgC in total), at a constant rate of a=2.52 PgC yr^{-1}. It is assumed that there is no decay of the biomass reservoir on this timescale. Following this scenario, we calculate 79 PgC (37 ppm) would have been removed from the atmosphere in 2035, 88 PgC (41 ppm) in 2050 giving RF(2050)≈ -0.49 W m^{-2}, and 94 PgC (44 ppm) in 2060, showing a saturation of the effect. Given that the 183 PgC stored in plantation biomass in 2060 exceeds estimates of the total amount of carbon that has been lost to date due to land use change (Houghton, 2008) (much of it from soil), it is not clear that it could be increased further. It has separately been estimated that 192 PgC could be accumulated in 50 years (Leake, 2008) but other sources give only 50–100 PgC (Winjum et al., 1992). Holding the 183 PgC store constant to 2100 (i.e. no further uptake or decay) causes the effect on the atmosphere to decay to 73 PgC (34 ppm), with RF(2100)≈ -0.37 W m^{-2}. Assuming strong mitigation, 35 PgC (16 ppm) are removed from the atmosphere in 3000 and RF$_{\text{final}}\approx -0.27$ W m^{-2}.

3.2.2 Bio-char production

It has been estimated that up to 0.56 PgC yr^{-1} of bio-char could be produced at present and that this could be significantly increased by up-scaling biomass energy production (Lehmann et al., 2006). One scenario for bio-char production suggests 15.6 PgC could be stored by 2035 and 52 PgC by 2060, increasing linearly at b=0.048 PgC yr^{-2} from 0 PgC yr^{-1} in 2010 to 1.2 PgC yr^{-1} in 2035 and then exponentially at c=1.5% yr^{-1} to

1.74 PgC yr^{-1} in 2060, i.e. approaching the size of the current land carbon sink (Read, 2008; Read and Parshotam, 2007). Assuming there is no decay of the charcoal carbon on this timescale, we calculate 11 PgC (5 ppm) would have been removed from the atmosphere in 2035, 22 PgC (10 ppm) in 2050 giving RF(2050)≈ -0.12 W m^{-2}, and 31 PgC (14 ppm) in 2060. There is scope to further scale-up this geoengineering option, according to estimates that if projected renewable energy demand in 2100 were met entirely through pyrolysis, up to 5.5–9.5 PgC yr^{-1} of bio-char could be produced (Lehmann et al., 2006). Continuing the exponential trend forward gives 3.15 PgC yr^{-1} in 2100, a total bio-char reservoir of 148 PgC and a corresponding removal from the atmosphere of 79 PgC (37 ppm) giving RF(2100)≈ -0.40 W m^{-2}. In the long term, the bio-char storage capacity of global cropland is estimated at 224 PgC and for temperate grasslands 175 PgC, i.e. $\sim$400 PgC in total (or a $\sim$25% increase in global soil carbon). Assuming that as it decays, this reservoir is continually refilled, the long-term potential is RF$_{\text{final}}\approx -0.52$ W m^{-2}, which in the strong mitigation scenario is due to a 34 ppm reduction in CO_2.

3.2.3 Air capture and storage

Bio-energy with carbon storage (BECS) is estimated to have a better cost-benefit ratio than air capture with sodium hydroxide (Keith et al., 2006). An optimistic estimate is that with CO_2 sequestration from fermentation starting in 2020 and CO_2 capture from flue gases in 2025, up to 50 PgC could be sequestered by 2035 and a whopping 298 PgC by 2060 (Read, 2008; Read and Parshotam, 2007). These figures assume that bio-fuels displace oil as the major transport fuels equivalent to 8.4 PgC yr^{-1} in 2035 and 12.2 PgC yr^{-1} in 2060, and biomass burning displaces a significant amount of the coal used in electricity production equivalent to 4.2 PgC yr^{-1} in 2035 and 6.1 PgC yr^{-1} in 2060. (These displacements are not considered here as they amount to mitigation.) Taking this scenario as an upper estimate we calculate that 124 PgC (58 ppm) would have been removed from the atmosphere in 2050, with

RF(2050)≈−0.69 W m^{-2}. Having reached such a high level, activity would be unlikely to just stop after 2060. Assuming sequestration remains constant at 11.8 PgC yr^{-1} until 2100, a massive 771 PgC would be sequestered causing a 399 PgC (186 ppm) atmospheric reduction and RF(2100)≈−1.99 W m^{-2}. Alternatively, chemical air capture with storage, using e.g. sodium hydroxide and lime, could potentially generate whatever size of carbon sink societies were willing to pay for, as it is unlikely to be limited by available substrates or land surface area (Keith et al., 2006). Ultimately the amount of CO_2 sequestered may be limited by the size of available geologic reservoirs, but their storage capacity is estimated to exceed available fossil fuel resources (IPCC, 2005; House et al., 2006). In the long term, air capture and storage activity appears to have the potential to sequester >1000 PgC and cancel the total emissions from a strong mitigation scenario, i.e. RF$_{final}$≈−1.43 W m^{-2}, and more.

3.2.4 Phosphorus addition to the ocean

Humans already mine and add to the land surface 0.39–0.45×10^{12} mol P yr^{-1} which has increased the riverine flux of biologically-available (dissolved and particulate) phosphorus (including sewage) to coastal seas by 0.27×10^{12} mol P yr^{-1}, suggesting a 60–70% transfer efficiency (Mackenzie et al., 2002). If all of this is converted to organic carbon with a Redfield ratio of C:P=106 then it is already generating a sink of 0.34 PgC yr^{-1}, mostly in coastal and shelf sea sediments. It has been suggested that mined phosphate could also be directly added to the surface ocean (Lampitt et al., 2008), potentially increasing the conversion efficiency to organic carbon. Regardless of whether this happens, we can expect inadvertent phosphorus additions to increase in future, one projection giving a linear increase to 0.42×10^{12} mol P yr^{-1} in 2035 (Mackenzie et al., 2002), which could drive a sink of 0.53 PgC yr^{-1}. Extrapolating the linear trend forwards gives 0.70×10^{12} mol P yr^{-1} added to the ocean in 2100 driving 0.88 PgC yr^{-1}. We calculate 14 PgC (6.5 ppm) removed from the atmosphere in 2050 giving RF(2050)≈−0.077 W m^{-2}, and 30 PgC (14 ppm) removed in 2100 giving

RF(2100)≈−0.15 W m^{-2}. On the millennial timescale, the total reservoir of mineable phosphate of 323–645×10^{12} mol P could readily be drained. Taking the upper estimate of the reservoir size, if 70% were to end up in bio-available form in the ocean and be converted to organic matter it would sequester 574 PgC giving RF$_{final}$≈−0.83 W m^{-2}, due to removing 112 PgC (52 ppm) in our strong mitigation scenario. This assumes that nitrogen fixation will cause nitrogen availability in the ocean to track increased phosphorus availability (Redfield, 1958; Lenton and Watson, 2000a) and that micronutrients (e.g. iron) do not limit new production in the (currently coastal) regions to which phosphate is added.

3.2.5 Ocean nitrogen fertilisation

There is a deficit of available nitrogen relative to phosphorus in the world ocean, of on average 2.7 μmol kg^{-1} (Anderson and Sarmiento, 1994), compared to an average deep ocean nitrate concentration of 30.9 μmol kg^{-1}. This deficit is maintained by negative feedbacks involving the processes of nitrogen fixation and denitrification (Lenton and Watson, 2000a), but it might be at least partly removed by alleviating iron (Falkowski, 1997) and/or phosphorus (Karl and Letelier, 2008) limitation of nitrogen fixation in low-nutrient low-chlorophyll (LNLC) regions (Lampitt et al., 2008). Removing the nitrogen deficit would result in a ∼9% (2.7/30.9) increase in the export flux. Estimates of the global export flux vary between methods, a recent model mean gives 17 PgC yr^{-1} at 75 m (Najjar et al., 2007), but the bottom of the photic zone is more typically taken to be 100 m where 11 PgC yr^{-1} has been estimated (Laws et al., 2000; Gehlen et al., 2006). This could be increased by about 1 PgC yr^{-1} by alleviating nitrogen limitation. However, what is critical for long term carbon storage is the sequestration flux below the depth of winter mixing, which ranges over 200–1000 m, depending on location (Lampitt et al., 2008). The sinking flux of carbon decays away with depth due to remineralisation, approximating a power law function (Martin et al., 1987), although the power is now known to vary significantly with surface community structure (Buesseler et al., 2007). If

we take 500 m as a reference depth, there the global sequestration flux is estimated to be in the range 2.3–5.5 PgC yr^{-1} (i.e. 20–50% of the export flux at 100 m) (Buesseler et al., 2007), with a long-favoured formula (Martin et al., 1987) giving 2.8 PgC yr^{-1} (i.e. 25% of the export flux). Sequestration at this depth would only be increased by 0.21–0.50 PgC yr^{-1} by alleviating nitrogen limitation. Using 0.5 PgC yr^{-1} as the upper limit for potential long-term sequestration due to global nitrogen fertilisation and starting at this constant level in 2020, then in 2050, 9.7 PgC (4.5 ppm) could be removed from the atmosphere and RF(2050)≈ -0.054 W m^{-2}, which in 2100 increases to 20 PgC (9.3 ppm) and RF(2100)≈ -0.10 W m^{-2}. In the long term, if the whole deficit of nitrogen in the global ocean could be removed and converted to carbon, assuming an ocean volume of 1.36×10^{18} m^3, a density of 1027 kg m^{-3} and a Redfield ratio of C:N$\sim$6.6, an additional 299 PgC might be stored in the deep ocean. However, at 0.5 PgC yr^{-1} it would take 600 years to achieve an additional 300 PgC of deep ocean storage. If this could be realised, then on the millennial timescale $RF_{final}\approx -0.38$ W m^{-2}, due to removing 54 PgC (25 ppm) in our strong mitigation scenario.

3.2.6 Ocean iron fertilisation

A number of model studies have assessed the potential carbon sink that could be generated by iron fertilisation of different high-nutrient low-chlorophyll (HNLC) areas of the world ocean (Aumount and Bopp, 2006; Jin et al., 2008; Zeebe and Archer, 2005). The maximum potential is indicated by simulations that remove iron limitation globally for 100 years in a model run forced with SRES A2 emissions (Aumount and Bopp, 2006). Global export production across 100 m is increased initially by 3.5 PgC yr^{-1}, decaying after 100 years to 1.8 PgC yr^{-1}, and totalling 226 PgC. This causes a 33 ppm reduction in atmospheric CO_2 from $\sim$800 ppm, equivalent to RF≈ -0.22 W m^{-2}. Diatoms are predicted to make a greater contribution to export production, creating fast sinking particles that should maximise the sequestration flux. If we take the predicted time mean increase in export flux across 100 m of 2.26 PgC yr^{-1}, and liken the remineralisation with depth to that at a station where diatoms dominate (K2 in the North-

west Pacific) (Buesseler et al., 2007), then we estimate an increase in sequestration flux across 500 m of 1 PgC yr^{-1}. If activity started at this level in 2020 we calculate that by 2050, 19 PgC (9 ppm) would be removed from the atmosphere, giving RF(2050)≈ -0.11 W m^{-2}, and by 2100, 40 PgC (19 ppm) would be removed from the atmosphere giving RF(2100)≈ -0.20 W m^{-2}. This is consistent with previous results (Aumount and Bopp, 2006) given our lower emissions scenario and the shorter interval of geoengineering – after 100 years of activity we estimate RF≈ -0.23 W m^{-2}. An earlier estimate that atmospheric CO_2 could be reduced by up to 15 ppm from a baseline of $\sim$700 ppm in 2100 (Zeebe and Archer, 2005), equates to a smaller RF≈ -0.11 W m^{-2}. On the millennial timescale, literature estimates of the extra carbon that could be stored in the deep ocean from alleviating iron limitation range over 106–227 PgC (Aumount and Bopp, 2006). The upper value translates to $RF_{final}\approx -0.29$ W m^{-2} due to removing 41 PgC (19 ppm) from the atmosphere in our strong mitigation scenario.

3.2.7 Enhance upwelling

For ocean pipes (Lovelock and Rapley, 2007) or pumps to work as a method of carbon sequestration they must bring up water that is enriched in nitrogen relative to carbon (assuming nitrogen is the limiting nutrient) (Lampitt et al., 2008), or bring up water enriched in phosphorus relative to carbon and trigger nitrogen fixation (Karl and Letelier, 2008). Concentrating on the first option, it is well established that nitrogen is preferentially remineralised from sinking organic matter relative to carbon, and the natural upwelling of this water is what allows net export of carbon to the deep ocean (i.e. the biological pump) to occur. Taking station ALOHA near Hawaii (in the North Pacific subtropical gyre) as representative of ocean gyres, approximately 20% of upwelling nitrate (and corresponding carbon export) is converted to a sequestration flux of carbon. Thus, if the upwelling flux into surface ocean gyres which all had and maintained complete nitrate utilisation could be enhanced by 1 Sv globally, assuming an average 30.9 μmol kg^{-1} of nitrate in the upwelling water (which means pipes from $\sim$500 m depth), the global export flux could increase by 0.08 PgC yr^{-1} (i.e. about 0.7%), but

the corresponding sequestration flux would only be ~0.016 PgC yr^{-1}. To achieve 1 Sv of upwelling would require 4.32 million pumps of the capacity proposed by Atmocean Inc. (http://www.atmocean.com/sequestration.htm). Assuming activity started in 2020, by 2050 0.3 PgC (0.1 ppm) could be removed from the atmosphere with a maximum RF(2050)≈−0.0017 W m^{-2}, whilst in 2100, 0.6 PgC (0.3 ppm) could be removed with a maximum RF(2100)≈−0.0032 W m^{-2}. Maintaining such activity to the end of the millennium gives RF_{final}≈−0.028 W m^{-2}, which in a strong mitigation scenario corresponds to removing 4.0 PgC (1.9 ppm).

3.2.8 Enhance downwelling

A range of methods aimed at increasing the North Atlantic Deep Water (NADW) production by 1 Sverdrup (Sv, 10^6 m^3 s^{-1}), from its current flow rate of 13–20 Sv, have been considered (Zhou and Flynn, 2005). This could be achieved by cooling surface waters by 1°C, by having large floating pumps that form and thicken sea ice. The increase in downwelling current has been estimated to lead to a net annual incremental flux of 0.0095 PgC yr^{-1} (Zhou and Flynn, 2005). Assuming activity starts in 2020, and that storage is permanent, and allowing for atmospheric adjustment, in 2050 a total of 0.18 PgC (0.08 ppm) would be removed from the atmosphere, giving a maximum RF(2050)≈−0.00095 W m^{-2}. If the activity continued to 2100, a total of 0.38 PgC (0.18 ppm) would be removed from the atmosphere, giving RF(2100)≈−0.0019 W m^{-2}. Even if activity continued to 3000, on a strong mitigation scenario only 2.4 PgC (1.1 ppm) would be removed from the atmosphere, giving RF_{final}≈−0.016 W m^{-2}. The actual value would be less as ocean storage is not permanent, and the method also has high costs (Zhou and Flynn, 2005).

3.2.9 Carbonate addition to the ocean

The alkalinity of the ocean could be increased by adding carbonate, thus increasing carbon uptake (Kheshgi, 1995). A detailed account has been presented based

on using a flotilla of ships to sprinkle finely ground limestone ($CaCO_3$) on areas of the surface ocean where the depth of the saturation horizon is shallow (250–500 m) and the upwelling velocity is large (30–300 m yr^{-1}) (Harvey, 2008). A sink of 0.27 PgC yr^{-1} has been calculated after a century of linearly ramping up activity, and if maintained for a further ~400 years it could reduce atmospheric CO_2 by ~30 ppm relative to a strong mitigation baseline of 450 ppm (Harvey, 2008), giving RF(2500)≈−0.36 W m^{-2}. In our strong mitigation scenario we calculate a weaker effect on atmospheric CO_2 of 36.2 PgC (17 ppm) removed in 2500 giving RF(2500)≈−0.20 W m^{-2}. On the way there, in 2050 0.9 PgC (0.4 ppm) are removed from the atmosphere and RF(2050)≈−0.0048 W m^{-2}, in 2100 4.9 PgC (2.3 ppm) are removed and RF(2100)≈−0.025 W m^{-2}. Assuming activity continued to 3000, a total of 251 PgC could be sequestered, removing 65 PgC (30 ppm) from the atmosphere in our strong mitigation scenario, and giving RF_{final}≈−0.46 W m^{-2}.

4 Discussion

Our results (Tables 1 and 2) are only as good as the input data and the assumptions that go into the calculations. Taking them at face value for now, we can compare the maximum radiative forcing potential of quite different climate geoengineering options, and contrast them with the radiative forcing due to anthropogenic CO_2 emissions, which even in a strong mitigation scenario will remain >1 W m^{-2} for the rest of the millennium, exceeding 3 W m^{-2} on the century timescale. Without mitigation, anthropogenic CO_2 forcing could reach ~7 W m^{-2} on the century timescale and remain >7 W m^{-2} on the millennial timescale. If we take 2100 as a time horizon for comparison and assume that the different shortwave geoengineering options could all be deployed on this timescale, we can rank the potential of the various options, grouping those of similar magnitude, but preserving the ordering of our estimates, and distinguishing distinct groups using

">", or "≫" where differences are of an order of magnitude:

Sunshades Stratospheric aerosols Cloud α mechanical	>	Air capture Desert α	>	Grassland α Cropland α Bio−char Afforestation	Fe fertilisation Settlement α P addition N fertilisation	≫	Carbonate addition Cloud α biological Urban α	≫	Upwelling Downwelling

Relatively few geoengineering options have the potential to counteract $>3\,W\,m^{-2}$ alone. Placing sunshades in space or increasing planetary albedo by injecting stratospheric aerosols appear to be the only options that can achieve a reasonably uniform $-3\,W\,m^{-2}$ and be scaled up if necessary. Increasing marine stratiform cloud albedo might achieve $-3\,W\,m^{-2}$ of globally averaged radiative forcing but the effects are necessarily more regional and patchy, so less good regional cancellation of longwave radiative forcing is to be expected. These measures all have relatively short lifetimes so need to be continually replenished to maintain their effects.

A couple of other measures could cancel $>1\,W\,m^{-2}$ alone. Air capture of CO_2, either by plants as bio-energy or by chemical means, followed by carbon storage could achieve $\sim -2\,W\,m^{-2}$ on the century timescale and has the advantage of acting globally. Greatly increasing the albedo of desert regions (if achievable) would be biased to those regions, and the albedo change (and hence the radiative forcing) achievable may have been grossly over-estimated.

If the estimates for the aforementioned options are seriously in error, or they were deemed unacceptable for other reasons, then a number of other options have potential magnitude $0.1–1\,W\,m^{-2}$. However, a combination of these would be required to counteract foreseeable anthropogenic radiative forcing, reminiscent of how the mitigation challenge has been broken down into a series of carbon "wedges" (Pacala and Socolow, 2004). Increasing the albedo of all grasslands and croplands together achieves $\sim -1\,W\,m^{-2}$, but it is unclear whether the $\sim -0.2\,W\,m^{-2}$ from increasing human settlement albedo can just be added to this, because there may be some overlap between what is classed as cropland and what is classed as human settlement. Afforestation combined with bio-char production could give $\sim -0.8\,W\,m^{-2}$. Combined global iron,

nitrogen and phosphorus fertilisation of the ocean might just achieve $\sim -0.45\,W\,m^{-2}$. If we could add up all these potential contributions (which is probably not valid), they would give a radiative forcing of $\sim -2.5\,W\,m^{-2}$, not enough to cancel the contribution of even strongly mitigated CO_2 emissions (and it would not be globally uniform).

Increasing ocean alkalinity, biologically enhancing cloud albedo in the Southern Ocean summer, or increasing the albedo of urban areas, could each only cancel less than 1% of the anticipated forcing on the century timescale, even under strong mitigation of CO_2 emissions (i.e. $<0.03\,W\,m^{-2}$). Enhancing ocean upwelling or downwelling have an order of magnitude weaker effect still.

On the nearer time horizon of 2050, a minimum atmospheric CO_2 of 450 ppm in the absence of geoengineering would give $\sim 2.6\,W\,m^{-2}$ radiative forcing, and combining all the upper estimates for carbon cycle geoengineering options (Table 2) gives $\sim -1.9\,W\,m^{-2}$. Thus, it would appear that only rapid, repeated, large-scale deployment of potent shortwave geoengineering options (e.g. stratospheric aerosols) could conceivably cool the climate to near its preindustrial state on the 2050 timescale. However, some carbon cycle geoengineering options could make a useful contribution of similar magnitude to identified mitigation "wedges" (Pacala and Socolow, 2004). In the most optimistic scenarios, air capture and storage by BECS, combined with afforestation and bio-char production appears to have the potential to remove ~ 100 ppm of CO_2 from the atmosphere giving $\sim -1.3\,W\,m^{-2}$. Combined iron, nitrogen and phosphorus fertilisation of the ocean can only achieve a maximum ~ 20 ppm CO_2 drawdown and $-0.24\,W\,m^{-2}$ on the 2050 timescale.

On the millennial timescale, the most potent options (sunshades, stratospheric aerosols, mechanically increasing marine cloud albedo, increasing desert albedo, and air capture and storage of CO_2) remain so. However, the ranking of the remaining

geoengineering options changes significantly:

$$\text{P addition} > \text{Grassland } \alpha > \begin{matrix}\text{Bio-char}\\ \text{Carbonate addition}\\ \text{Cropland } \alpha\end{matrix} > \begin{matrix}\text{N fertilisation}\\ \text{Fe fertilisation}\\ \text{Afforestation}\end{matrix} > \text{Settlement } \alpha \gg \begin{matrix}\text{Upwelling}\\ \text{Downwelling}\\ \text{Cloud } \alpha \text{ biological}\\ \text{Urban } \alpha\end{matrix}$$

After air capture and storage of liquid CO_2 (in sediments or geologic reservoirs), phosphorus addition to the ocean appears to offer the next largest long-term potential carbon store, and it is unique in that it will probably continue to happen inadvertently. Bio-char in soil offers the greatest potential for long-term carbon storage on land. These two options combined may have the potential to store nearly all the cumulative carbon emissions from a strong mitigation scenario (1000 PgC). Increasing ocean alkalinity goes from being ineffective on the century timescale to having a potentially significant role to play in climate cooling on the millennial timescale, as well as having a potentially valuable role to play in combating ocean acidification (Harvey, 2008). Nitrogen and iron fertilisation of the ocean may have greater long term potential for carbon storage than afforestation on land but they require centuries of sustained activity to achieve it (whereas the potential of afforestation and reforestation could be realised within this century).

Enhancing ocean upwelling or downwelling can be "knocked out" as global cooling options on any of the timescales we consider, unless either could greatly exceed the 1 Sv we have assumed. Biologically enhancing cloud albedo in the Southern Ocean summer can be knocked out as a global cooling option, but might be effective as a regional seasonal cooling option to protect Antarctic ice shelves (Wingenter et al., 2007). Urban albedo alteration can also be knocked out as a global cooling option, but it can play a potentially important role in reducing urban heat islands and improving air quality (Taha, 2008).

Some interesting comparisons between shortwave and longwave options in a given realm (land or ocean) emerge. Globally altering the albedo of all grasslands and croplands together may have greater cooling potential ($\sim -1\,\mathrm{W\,m^{-2}}$) than the combination of

afforestation/reforestation and adding bio-char to soil (~ -0.6 to $-0.8\,\mathrm{W\,m^{-2}}$, depending on the timescale). Mechanically enhancing marine stratiform cloud albedo appears to have a greater cooling potential than all ocean nutrient fertilisation measures combined. However, the longwave (CO_2) options act globally on the radiation balance whilst the shortwave options are regionally biased. Iron fertilisation of the Southern Ocean has $\sim -0.2\,\mathrm{W\,m^{-2}}$ global cooling potential but might generate up to $\sim -2\,\mathrm{W\,m^{-2}}$ regional cooling in summer via its effect on DMS emissions and cloud albedo (Wingenter et al., 2007).

On the face of it some encouraging results emerge from our analysis, but they come with very large caveats. We have examined maximum effects, which entail truly global deployment and may not be physically achievable (as upper limit values have generally been assumed). Deployment itself costs energy, which if obtained from fossil fuels would tend to counteract any reductions in radiative forcing achieved. For some options, e.g. adding calcium carbonate to the ocean, the CO_2 emissions of deployment could be of the same order as the CO_2 sink generated (Harvey, 2008). Generating the energy and materials required for global scale geoengineering in turn costs money, and we have ignored economic constraints.

If combined with strong mitigation, air capture of CO_2 by plants providing bio-energy, followed by carbon storage, might be able to return atmospheric CO_2 to pre-industrial levels sometime next century, thus removing the need for shortwave geoengineering to cool the climate beyond that time. Others have even argued that combining all land carbon cycle geoengineering options, atmospheric CO_2 could be brought back to the pre-industrial level within this century (Read, 2008; Read and Parshotam, 2007). However, if one examines the land areas involved in such scenarios (which we have adopted), they appear to be in conflict with food production and/or the preservation of natural ecosystems. Furthermore, arguments that such scenarios would generate revenue (Read, 2008; Read and Parshotam, 2007) appear questionable (Keith et al., 2006). In a model that includes the estimated costs of different technologies, which assumes air capture is implemented over 50 years, it makes little impression until late

this century with a sink of ~2 PgC yr^{-1} generated by 2100 (Keith et al., 2006), much smaller than we have assumed in the above calculations. Thus, we are sceptical about the feasibility or desirability of the BECS option, as currently framed. Concerns about land-use conflicts are largely eliminated by the chemical air capture and storage option, but its estimated costs are considerably higher (Keith et al., 2006). Putting economic concerns aside, the main feasibility constraint is the size and accessibility of geologic reservoirs for storing the captured CO_2.

Continual addition of phosphorus, nitrogen, iron and calcium carbonate to the ocean, if it could eliminate nitrogen and iron limitation and allow global export production to track increasing phosphorus input, could, when combined with strong mitigation, bring atmospheric CO_2 back to the pre-industrial level by the end of the millennium. However, this is a mammoth geoengineering task which would itself severely disrupt marine ecosystems, and we doubt whether the elimination of nitrogen limitation could be achieved. If these methods started to be successful and carbon export to depth increased significantly, it would generate widespread ocean anoxia as there would be no corresponding increase in oxygen supply. This in turn would be expected to trigger increased denitrification, removing nitrogen from the ocean and thus providing a strong negative feedback on increasing export production (Lenton and Watson, 2000a). Phosphorus addition generates a carbon sink in coastal seas where carbon is sequestered in sediments (rather than deep water), but this also entails eutrophication and potentially toxic algal blooms.

Land surface albedo modification methods appear to have a combined global potential of ~−3 W m^{-2} (Table 1), but are best considered as regional climate cooling options, because the actual forcing over the relevant regions would be much greater than this, which could lead to excessive regional cooling. The effectiveness of albedo modification methods depends greatly on the magnitude of albedo enhancement achievable and the area it is applied to, and we question some of the values proposed. Increasing the albedo of deserts by 0.44 essentially involves covering them up with a highly reflective material, but this would surely itself get covered in matter deposited from the

atmosphere, reducing its albedo or demanding regular cleaning and replacement. The assumption of 3.25 million km^2 of human settlement (Hamwey, 2007) appears questionable, given that urban areas are measured to cover less than a tenth of this. If realistic it must include many land surface types, probably dominated by pastures, for which an increase of albedo of 0.15 seems questionable given that a value of 0.04 is suggested for grasslands and croplands (Hamwey, 2007).

Turning to the ocean and proposals to mechanically enhance the albedo of marine stratiform clouds, all papers thus far (Bower et al., 2006; Latham, 2002; Latham et al., 2008) appear to have been based on under-estimates of the albedo change required to provide a given radiative forcing. Thus, revised calculations are required of the source flux of CCN required in different regions to give the necessary top-of-cloud albedo change, given the known saturating response of cloud albedo to adding CCN (Twomey, 1991). The atmosphere over the Southern Ocean is the most pristine in this respect and should exhibit the strongest response, yet recent reassessments of the biological approach to seasonally enhancing cloud albedo in this region (Woodhouse et al., 2008) suggest it may be a lot harder to achieve a given effect than originally assumed (Wingenter et al., 2007).

There are many other issues and caveats that should be considered in evaluating the various geoengineering proposals. In a separate paper (Vaughan and Lenton, 2009) we consider the side effects on other aspects of the Earth system, the timescales to develop and deploy different technologies, their reversibility and the rate at which their effects decay. For a good example of calculations of the cost and CO_2 emissions associated with deploying a specific option see (Harvey, 2008).

5 Conclusions

Climate geoengineering is best considered as a potential complement to the mitigation of CO_2 emissions, rather than as an alternative to it. Strong mitigation could achieve the equivalent of up to −4 W m^{-2} radiative forcing on the century timescale, relative

to a worst case scenario for rising CO_2. However, to tackle the remaining $3\,W\,m^{-2}$, which are likely even in a best case scenario of strongly mitigated CO_2, a number of geoengineering options show promise. Some shortwave geoengineering measures, most promisingly stratospheric aerosol injections, have the potential to roughly cancel mitigated CO_2 radiative forcing. Alternatively, a combination of land surface albedo modifications and mechanical enhancement of marine stratiform cloud albedo, could achieve a patchy or partial cancellation of mitigated CO_2 radiative forcing. However, most shortwave options carry a heavy burden of risk because they have to be continually replenished and if deployment is suddenly stopped, extremely rapid warming could ensue. Carbon cycle geoengineering carries less risk associated with failure and some options appear to have the unique potential to return CO_2 to its pre-industrial level within a couple of centuries, which will not happen naturally, even on a millennial timescale. Air capture and storage shows the greatest potential, potentially combined with afforestation/reforestation and bio-char production. If our estimates are even remotely accurate, recent interest in ocean carbon cycle geoengineering seems a little misplaced, because even the more promising options are only worth considering as a millennial timescale activity. Perhaps the most surprising result is that activities that are already underway, particularly inadvertent phosphorus addition to coastal and shelf seas, may have greater long-term carbon sequestration potential than the much-studied iron fertilisation. Some other suggestions that have received considerable media attention, in particular "ocean pipes" appear to be ineffective. The real value of such suggestions has been to redirect attention to the whole topic area. We hope that the present contribution provides a useful quantitative first step that can inform the prioritisation of further research into various climate geoengineering options, and provide a common framework for the evaluation of new proposals.

Appendix A

Solutions for CO_2 removed from the atmosphere

Letting $\Delta t = t_f - t$ and inserting Eqs. (11) and (12) into (13) gives:

$$\begin{aligned}\Delta C_{\text{atm}} &= -\int_{t_s}^{t_c} R(t) g(t_f - t) f(t_f - t)\,dt \\ &= -\int_{t_s}^{t_c} R(t) \left(\begin{array}{l} 0.18e^{\frac{(t-t_f)}{\tau}} + 0.14e^{(t-t_f)\left(\frac{1}{\tau}+\frac{1}{420}\right)} + 0.18e^{(t-t_f)\left(\frac{1}{\tau}+\frac{1}{70}\right)} \\ +0.24e^{(t-t_f)\left(\frac{1}{\tau}+\frac{1}{21}\right)} + 0.26e^{(t-t_f)\left(\frac{1}{\tau}+\frac{1}{3.4}\right)} \end{array} \right) dt \end{aligned} \quad \text{(A1)}$$

Alternatively, assuming permanent sequestration, $g(t_f - t) = 1$:

$$\begin{aligned}\Delta C_{\text{atm}} &= -\int_{t_s}^{t_c} R(t) f\,(t_f - t)\,dt \\ &= -\int_{t_s}^{t_c} R(t) \left(0.18 + 0.14e^{(t-t_f)/420} + 0.18e^{(t-t_f)/70} + 0.24e^{(t-t_f)/21} + 0.26e^{(t-t_f)/3.4}\right) dt \end{aligned} \quad \text{(A2)}$$

The presentation is simplified if we define the start time of geoengineering action, $t_s = 0$. We then consider 3 cases for the geoengineering carbon removal function, $R(t)$:

(a) Constant removal $R(t) = a$ (in $PgC\,yr^{-1}$) is the simplest case:

$$\begin{aligned}\Delta C_{\text{atm}} &= -\int_0^{t_c} R(t) g(t_f - t) f(t_f - t)\,dt = -a\int_0^{t_c} g(t_f - t) f(t_f - t)\,dt \\ &= -a \left(\begin{array}{l} 0.18\tau\left(e^{\frac{(t_c - t_f)}{\tau}} - e^{-\frac{t_f}{\tau}}\right) + \frac{0.14}{\left(\frac{1}{\tau}+\frac{1}{420}\right)}\left(e^{(t_c - t_f)\left(\frac{1}{\tau}+\frac{1}{420}\right)} - e^{-t_f\left(\frac{1}{\tau}+\frac{1}{420}\right)}\right) \\ + \frac{0.18}{\left(\frac{1}{\tau}+\frac{1}{70}\right)}\left(e^{(t_c - t_f)\left(\frac{1}{\tau}+\frac{1}{70}\right)} - e^{-t_f\left(\frac{1}{\tau}+\frac{1}{70}\right)}\right) + \frac{0.24}{\left(\frac{1}{\tau}+\frac{1}{21}\right)}\left(e^{(t_c - t_f)\left(\frac{1}{\tau}+\frac{1}{21}\right)} - e^{-t_f\left(\frac{1}{\tau}+\frac{1}{21}\right)}\right) \\ + \frac{0.26}{\left(\frac{1}{\tau}+\frac{1}{3.4}\right)}\left(e^{(t_c - t_f)\left(\frac{1}{\tau}+\frac{1}{3.4}\right)} - e^{-t_f\left(\frac{1}{\tau}+\frac{1}{3.4}\right)}\right) \end{array} \right) \end{aligned} \quad \text{(A3)}$$

In the case of permanent sequestration, $g(t_f - t)$=1:

$$\Delta C_{\text{atm}} = -a\int_0^{t_c} f(t_f - t)dt$$
$$= -a\left(\begin{array}{l} 0.18t_c + 58.8\left(e^{\frac{(t_c-t_f)}{420}} - e^{-\frac{t_f}{420}}\right) + 12.6\left(e^{\frac{(t_c-t_f)}{70}} - e^{-\frac{t_f}{70}}\right) \\ +5.04\left(e^{\frac{(t_c-t_f)}{21}} - e^{-\frac{t_f}{21}}\right) + 0.884\left(e^{\frac{(t_c-t_f)}{3.4}} - e^{-\frac{t_f}{3.4}}\right) \end{array}\right) \quad \text{(A4)}$$

(b) Linearly increasing removal with time $R(t)=bt$, where b (in PgC yr^{-2}) is the rate of increase in removal, requires integration by parts and gives:

$$\Delta C_{\text{atm}} = -\int_0^{t_c} R(t)g(t_f - t)f(t_f - t)dt = -b\int_0^{t_c} tg(t_f - t)f(t_f - t)dt$$
$$= -b\left(\begin{array}{l} 0.18\tau e^{\frac{(t_c-t_f)}{\tau}}(t_c-\tau)+0.18\tau^2 e^{-\frac{t_f}{\tau}} + \frac{0.14}{\left(\frac{1}{\tau}+\frac{1}{420}\right)}e^{(t_c-t_f)\left(\frac{1}{\tau}+\frac{1}{420}\right)}\left(t_c - \frac{1}{\left(\frac{1}{\tau}+\frac{1}{420}\right)}\right) \\ + \frac{0.14}{\left(\frac{1}{\tau}+\frac{1}{420}\right)^2}e^{-t_f\left(\frac{1}{\tau}+\frac{1}{420}\right)} + \frac{0.18}{\left(\frac{1}{\tau}+\frac{1}{70}\right)}e^{(t_c-t_f)\left(\frac{1}{\tau}+\frac{1}{70}\right)}\left(t_c - \frac{1}{\left(\frac{1}{\tau}+\frac{1}{70}\right)}\right) \\ + \frac{0.18}{\left(\frac{1}{\tau}+\frac{1}{70}\right)^2}e^{-t_f\left(\frac{1}{\tau}+\frac{1}{70}\right)} + \frac{0.24}{\left(\frac{1}{\tau}+\frac{1}{21}\right)}e^{(t_c-t_f)\left(\frac{1}{\tau}+\frac{1}{21}\right)}\left(t_c - \frac{1}{\left(\frac{1}{\tau}+\frac{1}{21}\right)}\right) \\ + \frac{0.24}{\left(\frac{1}{\tau}+\frac{1}{21}\right)^2}e^{-t_f\left(\frac{1}{\tau}+\frac{1}{21}\right)} + \frac{0.26}{\left(\frac{1}{\tau}+\frac{1}{3.4}\right)}e^{(t_c-t_f)\left(\frac{1}{\tau}+\frac{1}{3.4}\right)}\left(t_c - \frac{1}{\left(\frac{1}{\tau}+\frac{1}{3.4}\right)}\right) \\ + \frac{0.26}{\left(\frac{1}{\tau}+\frac{1}{3.4}\right)^2}e^{-t_f\left(\frac{1}{\tau}+\frac{1}{3.4}\right)} \end{array}\right) \quad \text{(A5)}$$

2597

In the case of permanent sequestration, $g(t_f - t)$=1:

$$\Delta C_{\text{atm}} = -b\int_0^{t_c} tf(t_f - t)dt$$
$$= -b\left(\begin{array}{l} 0.09t_c^2 + 58.8t_c e^{\frac{(t_c-t_f)}{420}} + 24696\left(e^{-\frac{t_f}{420}} - e^{\frac{(t_c-t_f)}{420}}\right) + 12.6t_c e^{\frac{(t_c-t_f)}{70}} \\ +882\left(e^{-\frac{t_f}{70}} - e^{\frac{(t_c-t_f)}{70}}\right) + 5.04t_c e^{\frac{(t_c-t_f)}{21}} + 105.84\left(e^{-\frac{t_f}{21}} - e^{\frac{(t_c-t_f)}{21}}\right) \\ +0.884t_c e^{\frac{(t_c-t_f)}{3.4}} + 3.0056\left(e^{-\frac{t_f}{3.4}} - e^{\frac{(t_c-t_f)}{3.4}}\right) \end{array}\right) \quad \text{(A6)}$$

(c) Exponentially increasing removal with time, $R(t)=R_0e^{ct}$, where R_0 (in PgC yr^{-1}) is the initial removal rate and c (yr^{-1}) is the fractional rate of increase in geoengineering activity, gives:

$$\Delta C_{\text{atm}} = -\int_0^{t_c} R\,(t)\,g\,(t_f - t)\,f\,(t_f - t)dt = -R_0\int_0^{t_c} e^{ct}g\,(t_f - t)\,f\,(t_f - t)dt$$
$$= -R_0\left(\begin{array}{l} \frac{0.18}{\left(c+\frac{1}{\tau}\right)}\left(e^{\left(c+\frac{1}{\tau}\right)t_c - \frac{t_f}{\tau}} - e^{-\frac{t_f}{\tau}}\right) + \frac{0.14}{\left(c+\frac{1}{\tau}+\frac{1}{420}\right)}\left(e^{\left(c+\frac{1}{\tau}+\frac{1}{420}\right)t_c - \left(\frac{1}{\tau}+\frac{1}{420}\right)t_f} - e^{-\left(\frac{1}{\tau}+\frac{1}{420}\right)t_f}\right) \\ + \frac{0.18}{\left(c+\frac{1}{\tau}+\frac{1}{70}\right)}\left(e^{\left(c+\frac{1}{\tau}+\frac{1}{70}\right)t_c - \left(\frac{1}{\tau}+\frac{1}{70}\right)t_f} - e^{-\left(\frac{1}{\tau}+\frac{1}{70}\right)t_f}\right) \\ + \frac{0.24}{\left(c+\frac{1}{\tau}+\frac{1}{21}\right)}\left(e^{\left(c+\frac{1}{\tau}+\frac{1}{21}\right)t_c - \left(\frac{1}{\tau}+\frac{1}{21}\right)t_f} - e^{-\left(\frac{1}{\tau}+\frac{1}{21}\right)t_f}\right) \\ + \frac{0.26}{\left(c+\frac{1}{\tau}+\frac{1}{3.4}\right)}\left(e^{\left(c+\frac{1}{\tau}+\frac{1}{3.4}\right)t_c - \left(\frac{1}{\tau}+\frac{1}{3.4}\right)t_f} - e^{-\left(\frac{1}{\tau}+\frac{1}{3.4}\right)t_f}\right) \end{array}\right) \quad \text{(A7)}$$

In the case of permanent sequestration, $g(t_f - t)$=1:

$$\Delta C_{\text{atm}} = -R_0\int_0^{t_c} e^{ct}f(t_f - t)dt$$
$$= -R_0\left(\begin{array}{l} \frac{0.18}{c}\left(e^{ct_c} - 1\right) + \frac{0.14}{\left(c+\frac{1}{420}\right)}\left(e^{ct_c + \frac{(t_c-t_f)}{420}} - e^{-\frac{t_f}{420}}\right) + \frac{0.18}{\left(c+\frac{1}{70}\right)}\left(e^{ct_c + \frac{(t_c-t_f)}{70}} - e^{-\frac{t_f}{70}}\right) \\ + \frac{0.24}{\left(c+\frac{1}{21}\right)}\left(e^{ct_c + \frac{(t_c-t_f)}{21}} - e^{-\frac{t_f}{21}}\right) + \frac{0.26}{\left(c+\frac{1}{3.4}\right)}\left(e^{ct_c + \frac{(t_c-t_f)}{3.4}} - e^{-\frac{t_f}{3.4}}\right) \end{array}\right) \quad \text{(A8)}$$

These solutions can readily be combined for removal scenarios that have different phases using different removal functions drawn from cases (a)–(c).

Acknowledgements. We thank Jim Lovelock for inspiring TML to think about the topic and Andy Watson, Phil Williamson and Phil Goodwin for comments on earlier drafts. We thank the organisers and participants of the 38th Session of the International Seminar on Nuclear War and Planetary Emergencies in Erice, Italy, August 2007 and of the Workshop on Earth System Engineering in Wilbad Kreuth, Germany, September 2008 for stimulating discussions on climate geoengineering. TML's contribution is part of the "Feedbacks QUEST" project of the Natural Environment Research Council (NE/F001657/1). NEV is a Tyndall PhD student funded by the School of Environmental Sciences.

References

Akbari, H., Menson, S., and Rosenfeld, A.: Global Cooling: Increasing world-wide urban albedos to offset CO_2, Climatic Change, doi:10.1007/s10584-008-9515-9, 2008.

Anderson, L. A. and Sarmiento, J. L.: Redfield ratios of remineralization determined by nutrient data analysis, Global Biogeochem. Cy., 8, 65–80, 1994.

Angel, R.: Feasibility of cooling the earth with a cloud of small spacecraft near the inner Lagrange point (l1), Proc. Natl. Acad. Sci. USA, 103, 17 184–17 189, 2006.

Aumount, O. and Bopp, L.: Globalizing results from ocean in situ iron fertilization studies, Global Biogeochem. Cy., 20, GB2017, doi:10.1029/2005GB002591, 2006.

Bower, K., Choularton, T., Latham, J., Sahraei, J., and Salter, S.: Computational assessment of a proposed technique for global warming mitigation via albedo enhancement of marine stratocumulus clouds, Atmos. Res., 82, 328–336, 2006.

Boyd, P. W.: Ranking geo-engineering schemes, Nature Geoscience, 1, 722–724, 2008.

Buesseler, K. O., Lamborg, C. H., Boyd, P. W., Lam, P. J., Trull, T. W., Bidigare, R. R., Bishop, J. K. B., Casciotti, K. L., Dehairs, F., Elskens, M., Honda, M., Karl, D. M., Siegel, D. A., Silver, M. W., Steinberg, D. K., Valdes, J., Van Mooy, B., and Wilson, S.: Revisiting Carbon Flux Through the Ocean's Twilight Zone, Science, 316, 567–570, 2007.

Canadell, J. G., LeQuere, C., Raupach, M. R., Field, C. B., Buitenhuis, E. T., Ciais, P., Conway, T. J., Gillett, N. P., Houghton, R. A., and Marland, G.: Contributions to accelerating atmospheric CO_2 growth from economic activity, carbon intensity, and efficiency of natural sinks, Proc. Natl. Acad. Sci. USA, 104, 18 866–18 870, 2007.

Charlson, R. J., Lovelock, J. E., Andreae, M. O., and Warren, S. G.: Oceanic phytoplankton, atmospheric sulphur, cloud albedo and climate, Nature, 326, 655–661, 1987.

Cox, P. M., Betts, R. A., Jones, C. D., Spall, S. A., and Totterdell, I. J.: Acceleration of global warming due to carbon-cycle feedbacks in a coupled climate model, Nature, 408, 184–187, 2000.

Crutzen, P. J.: Albedo enhancement by stratospheric sulphur injections: A contribution to resolve a policy dilemma?, Climatic Change, 77, 211–219, 2006.

Falkowski, P. G.: Evolution of the nitrogen cycle and its influence on the biological sequestration of CO_2 in the ocean, Nature, 387, 272–275, 1997.

Friedlingstein, P., Cox, P., Betts, R., Bopp, L., Bloh, W. v., Brovkin, V., Doney, S., Eby, M., Fung, I., Govindasamy, B., John, J., Jones, C., Joos, F., Kato, T., Kawamiya, M., Knorr, W., Lindsay, K., Matthews, H. D., Raddatz, T., Rayner, P., Reick, C., Roeckner, E., Schnitzler, K.-G., Schnur, R., Strassmann, K., Thompson, S., Weaver, A. J., Yoshikawa, C., and Zeng, N.: Climate-carbon cycle feedback analysis: Results from the C4MIP model intercomparison, J. Climate, 19, 3337–3353, 2006.

Gaskill, A.: Summary of Meeting with US DOE to discuss Geoengineering options to prevent abrupt and long-term climate change, available at: http://www.global-warming-geo-engineering.org/DOE-Meeting/DOE-Geoengineering-Climate-Change-Meeting/ag1.html (last access: 20 January 2009), 2004.

Gehlen, M., Bopp, L., Emprin, N., Aumont, O., Heinze, C., and Ragueneau, O.: Reconciling surface ocean productivity, export fluxes and sediment composition in a global biogeochemical ocean model, Biogeosciences, 3, 521–537, 2006, http://www.biogeosciences.net/3/521/2006/.

Govindasamy, B. and Caldeira, K.: Geoengineering Earth's radiation balance to mitigate CO_2-induced climate change, Geophys. Res. Lett., 27, 2141–2144, 2000.

Hamwey, R. M.: Active amplification of the terrestrial albedo to mitigate climate change: An exploratory study, Mitigation and Adaptation Strategies for Global Change, 12, 419–439, 2007.

Hansen, M. C., DeFries, R. S., Townshend, J. R. G., and Sohlberg, R.: Global land cover classification at 1 km spatial resolution using a classification tree approach, Int. J. Remote Sens., 21, 1331–1364, 2000.

Harvey, L. D. D.: Mitigating the atmospheric CO_2 increase and ocean acidification by adding limestone powder to upwelling regions, J. Geophys. Res.-Oceans, 113, C04028, doi:10.1029/2007JC004373, 2008.

Houghton, R. A.: Carbon Flux to the Atmosphere from Land-Use Changes: 1850–2005, in: TRENDS: A Compendium of Data on Global Change, Carbon Dioxide Information Analysis Center, Oak Ridge National Laboratory, US Department of Energy, Oak Ridge, Tennesee, USA, 2008.

House, K. Z., Schrag, D. P., Harvey, C. F., and Lackner, K. S.: Permanent carbon dioxide storage in deep-sea sediments, Proc. Natl. Acad. Sci. USA, 103, 12 291–12 295, 2006.

IPCC: Climate Change 2001: The Scientific Basis, Cambridge University Press, Cambridge, 881 pp., 2001.

IPCC: Carbon Dioxide Capture and Storage, Cambridge University Press, Cambridge, 442 pp., 2005.

IPCC: Climate Change 2007: The Physical Science Basis, Cambridge University Press, Cambridge, 996 pp., 2007.

Jin, M., Dickinson, R. E., and Zhang, D.-L.: The Footprint of Urban Areas on Global Climate as Characterized by MODIS, J. Climate, 18, 1551–1565, 2005.

Jin, X., Gruber, N., Frenzel, H., Doney, S. C., and McWilliams, J. C.: The impact on atmospheric CO_2 of iron fertilization induced changes in the ocean's biological pump, Biogeosciences, 5, 385–406, 2008, http://www.biogeosciences.net/5/385/2008/.

Joos, F., Bruno, M., Fink, R., Siegenthaler, U., Stocker, T. F., LeQuere, C., and Sarmiento, J. L.: An efficient and accurate representation of complex oceanic and biospheric models of anthropogenic carbon uptake, Tellus B, 48, 397–417, 1996.

Karl, D. M. and Letelier, R.: Nitrogen fixation-enhanced carbon sequestration in low nitrate, low chlorophyll seascapes, Mar. Ecol.-Prog. Ser., 364, 257–268, 2008.

Keith, D. W., Ha-Doung, M., and Stolaroff, J. K.: Climate strategy with CO_2 capture from the air, Climatic Change, 74, 17–45, 2006.

Kharecha, P. A. and Hansen, J. E.: Implications of "peak oil" for atmospheric CO_2 and climate, Global Biogeochem. Cy., 22, GB3012, 2008.

Kheshgi, H. S.: Sequestering Atmospheric carbon dioxide by increasing ocean alkalinity, Energy, 20, 915–922, 1995.

Kiehl, J. T. and Trenberth, K. E.: Earth's annual global mean energy budget, B. Am. Meteorol. Soc., 78, 197–208, 1997.

Lampitt, R. S., Achterberg, E. P., Anderson, T. R., Hughes, J. A., Iglesias-Rodriguez, M. D., Kelly-Gerreyn, B. A., Lucas, M., Popove, E. E., Sanders, R., Shepherd, J. G., Smythe-Wright, D., and Yool, A.: Ocean fertilization: a potential means of geoengineering, Philos. T. R. Soc. A, 366(1882), 3919–3945, doi:10.1098/rsta.2008.0139, 2008.

Latham, J.: Control of global warming?, Nature, 347, 339–340, 1990.

Latham, J.: Amelioration of global warming by controlled enhancement of the albedo and longevity of low-level maritime clouds, Atmospheric Science Letters, 3, 52–58, 2002.

Latham, J., Rasch, P., Chen, C.-C., Kettles, L., Gadian, A., Gettelman, A., Morrison, H., Bower, K., and Choularton, T.: Global temperature stabilization via controlled albedo enhancement of low-level maritime clouds, Philos. T. R. Soc. A, 366(1882), 3969–3987, doi:10.1098/rsta.2008.0137, 2008.

Laws, E. A., Falkowski, P. G., Smith, W. O., Ducklow, H., and McCarthy, J. J.: Temperature effects on export production in the open ocean, Global Biogeochem. Cy., 14, 1231–1246, 2000.

Leake, J. E.: "Biosphere carbon stock management: Addressing the threat of abrupt climate change in the next few decades." By Peter Read, An editorial comment., Climatic Change, 87, 329–334, 2008.

Lehmann, J., Gaunt, J., and Rondon, M.: Bio-char sequestration in terrestrial ecosystems – a review, Mitigation and Adaptation Strategies for Global Change, 11, 403–427, 2006.

Lenton, T. M.: Land and ocean carbon cycle feedback effects on global warming in a simple Earth system model, Tellus B, 52, 1159–1188, doi:10.1034/j.1600-0889.2000.01104.x, 2000.

Lenton, T. M. and Watson, A. J.: Redfield revisited: 1. Regulation of nitrate, phosphate and oxygen in the ocean, Global Biogeochem. Cy., 14, 225–248, 2000a.

Lenton, T. M.: Climate Change to the end of the Millennium, Climatic Change, 76, 7–29, doi:10.1007/s10584-005-9022-1, 2006.

Loveland, T. R., Reed, B. C., Brown, J. F., Ohlen, D. O., Zhu, Z., Yang, L., and Merchant, J. W.: Development of a global land cover characteristics database and IGBP DISCover from 1 km AVHRR data, Int. J. Remote Sens., 21, 1303–1330, 2000.

Lovelock, J. E. and Rapley, C. G.: Ocean pipes could help the earth to cure itself, Nature, 449, p. 403, 2007.

MacCracken, M. C.: Geoengineering: Worthy of cautious evaluation?, Climatic Change, 77, 235–243, 2006.

Mackenzie, F. T., Ver, L. M., and Lerman, A.: Century-scale nitrogen and phosphorus controls of the carbon cycle, Chem. Geol., 190, 13–32, 2002.

Martin, J. H., Knauer, G. A., Karl, D. M., and Broenkow, W. W.: VERTEX: Carbon cycling in the northeast Pacific, Deep Sea-Res., 34, 267–285, 1987.

Najjar, R. G., Jin, X., Louanchi, F., Aumont, O., Caldeira, K., Doney, S. C., Dutay, J.-C., Follows, M., Gruber, N., Joos, F., Lindsay, K., Maier-Reimer, E., Matear, R. J., Matsumoto, K., Monfray, P., Mouchet, A., Orr, J. C., Plattner, G.-K., Sarmiento, J. L., Schlitzer, R., Slater, R. D., Weirig, M.-F., Yamanaka, Y., and Yool, A.: Impact of circulation on export production, dissolved organic matter, and dissolved oxygen in the ocean: Results from Phase II of the Ocean Carbon-cycle Model Intercomparison Project (OCMIP-2), Global Biogeochem. Cy., 21, GB3007, 10.1029/2006GB002857, 2007.

NAS: Policy Implications of Greenhouse Warming: Mitigation, Adaptation, and the Science Base, Washington, DC, 918 pp., 1992.

Oman, L., Robock, A., Stenchikov, G. L., Schmidt, G. A., and Ruedy, R.: Climatic response to high-latitude volcanic eruptions, J. Geophys. Res.-Atmos., 110, D13103, doi:10.1029/2004JD005487, 2005.

Pacala, S. and Socolow, R.: Stabilization Wedges: Solving the Climate Problem for the Next 50 Years with Current Technologies, Science, 305, 968–972, 2004.

Pearson, J., Oldson, J., and Levin, E.: Earth rings for planetary environment control, Acta astronaut., 58, 44–57, 2006.

Rasch, P. J., Crutzen, P. J., and Coleman, D. B.: Exploring the geoengineering of climate using stratospheric sulphate aerosols: The role of particle size, Geophys. Res. Lett., 35, L02809, doi:10.1029/2007GL032179, 2008.

Raupach, M. R., Marland, G., Ciais, P., LeQuere, C., Canadell, J. G., Klepper, G., and Field, C. B.: Global and regional drivers of accelerating CO_2 emissions, Proceedings of the National Academy of Science, 104, 10 288–10 293, 2007.

Read, P. and Lermit, J.: Bio-energy with carbon storage (BECS): A sequential decision approach to the threat of abrupt climate change, Energy, 30, 2654–2671, 2005.

Read, P. and Parshotam, A.: Holistic greenhouse gas management strategy (with reviewers' comments and authors' rejoinders), Victoria University of Wellington, Wellington, New Zealand, available at: http://ips.ac.nz/publications/publications/show/205 (last access: 20 January 2009), 2007.

Read, P.: Biosphere carbon stock management: addressing the threat of abrupt climate change in the next few decades: an editorial essay, Climatic Change, 87, 305–320, 2008.

Redfield, A. C.: The biological control of chemical factors in the environment, Am. Sci., 46, 205–221, 1958.

Ridgwell, A., Singarayer, J. S., Hetherington, A. M., and Valdes, P. J.: Tackling regional climate change by leaf albedo bio-geoengineering, Curr. Biol., 19, doi:10.1016/j.cub.2008.12.025, 2009.

Robock, A., Oman, L., and Stenchikov, G. L.: Regional climate responses to geoengineering with tropical and Arctic SO_2 injections, J. Geophys. Res.-Atmos., 113, D16101, doi:10.1029/2008JD010050, 2008.

Rosenfeld, A. H., Romm, J. J., Akbari, H., and LLoyd, A. C.: Painting the town white and green, Technol. Rev., 100, 52–59, 1997.

Stenchikov, G. L., Kirchner, I., Robock, A., Graf, H. F., Antuna, J. C., Grainger, R. G., Lambert, A., and Thomason, L.: Radiative forcing from the 1991 mount Pinatubo volcanic eruption, J. Geophys. Res.-Atmos., 103, 13 837–13 857, 1998.

Stern, N.: The Economics of Climate Change: The Stern Review, Cambridge University Press, Cambrige, 692 pp., 2006.

Taha, H.: Urban surface modification as a potential ozone air-quality improvement strategy in California: a mesoscale modelling study, Bound.-Lay. Meteorol., 127, 219–239, 2008.

Teller, E., Wood, L., and Hyde, R.: Global Warming and Ice Ages: I. Prospects For Physics Based Modulation of Global Change, Lawrence Livermore National Laboratory (LLNL), CA (USA), Preprint UCRL-JC-128715, 1997.

Teller, E., Hyde, R., and Wood, L.: Active Climate Stabilization: Practical Physics-Based Approaches to Prevention of Climate Change, Lawrence Livermore National Laboratory (LLNL), CA (USA), Preprint UCRL-JC-148012, 2002.

Tsvetsinskaya, E. A., Schaaf, C. B., Gao, F., Strahler, A. H., Dickinson, R. E., Zeng, X., and Lucht, W.: Relating MODIS-derived surface albedo to soils and rock types over Northern Africa and the Arabian peninsula, Geophys. Res. Lett., 29, 1353, doi:10.1029/2001GL014096, 2002.

Twomey, S.: Aerosols, clouds and radiation, Atmos. Environ., 25A, 2435–2442, 1991.

Vaughan, N. E. and Lenton, T. M.: A review of climate geoengineering proposals, Climatic Change, submitted, 2009.

Vogt, M., Vallina, S., and von Glasow, R.: New directions: Correspondence on "enhancing the natural cycle to slow global warming", Atmos. Environ., 42, 4803–4805, 2008.
Wigley, T. M. L.: A combined mitigation/geoengineering approach to climate stabilization, Science, 314, 452–454, 2006.
Wingenter, O. W., Elliot, S. M., and Blake, D. R.: New directions: Enhancing the natural sulphur cycle to slow global warming, Atmos. Environ., 41, 7373–7375, 2007.
Winjum, J. K., Dixon, R. K., and Schroeder, P. E.: Estimating the global potential of forest and agroforest management practices to sequester carbon, Water Air Soil Poll., 64, 213–227, 1992.
Woodhouse, M. T., Mann, G. W., Carslaw, K. S., and Boucher, O.: New Directions: The impact of oceanic iron fertilisation on cloud condensation nuclei, Atmos. Environ., 42, 5728–5730, 2008.
Zeebe, R. E. and Archer, D.: Feasibility of ocean fertilization and its impact on future atmospheric CO_2 levels, Geophys. Res. Lett., 32, L09703, doi:10.1029/2005GL022449, 2005.
Zeman, F.: Energy and material balance of CO_2 capture from ambient air, Environ. Sci. Technol., 41, 7558–7563, 2007.
Zhou, S. and Flynn, P. C.: Geoengineering downwelling ocean currents: A cost assessment, Climatic Change, 71, 203–220, 2005.

Table 1. Estimated radiative forcing potential of geoengineering options to alter planetary albedo. In common with the literature, for the first two options, back calculations are made of the albedo change required to counteract the radiative forcing due to doubling CO_2, whereas for the remaining options, forward calculations are made of the maximum potential radiative forcing. The latter are based on upper limit albedo changes and areas suggested in the literature (see text). Calculations were done at full precision but outputs are generally given to 2 significant figures commensurate with our first order approach.

Option	Area	Fraction of Earth	Proposed albedo change within area	Scaled albedo change of layer	Eq. used	Planetary albedo change	RF
	(m^2)	f_{Earth}				$\Delta\alpha_p$	($W\,m^{-2}$)
Increase atmospheric albedo				$\Delta\alpha_a$			
Stratospheric aerosols	5.1×10^{14}	1	0.012	0.012	(4)	0.011	−3.71
Cloud albedo – mechanical	8.9×10^{13}	0.175	0.091	0.016	(6)	0.011	−3.71
Cloud albedo – biological	5.1×10^{13}	0.1	0.008	0.000067*	(6)	0.000045	−0.016
Increase surface albedo				$\Delta\alpha_s$			
Desert	1.0×10^{13}	0.02	0.44	0.0088	(7)	0.0051	−1.74
Grassland	3.85×10^{13}	0.075	0.0425	0.0032	(7)	0.0019	−0.64
Cropland	1.4×10^{13}	0.028	0.08	0.0022	(7)	0.0013	−0.44
Human settlement	3.25×10^{12}	0.0064	0.15	0.00096	(7)	0.00055	−0.19
Urban areas	2.6×10^{11}	0.00051	0.1	0.000051	(7)	0.000030	−0.010

* Biological enhancement of cloud albedo is only applied for 1 month per year hence division by 12.

Table 2. Estimated maximum radiative forcing potential of carbon cycle geoengineering options. Effects are calculated relative to a strong mitigation scenario in which a total of 1000 PgC are emitted and atmospheric CO_2 (and corresponding radiative forcing) reaches 450 ppm (2.58 W m^{-2}) in 2050, stabilises at 500 ppm (3.14 W m^{-2}) in 2100 and then declines to 363 ppm (1.43 W m^{-2}) on a millennial timescale.

Option	2050		2100			3000	
	ΔCO_2 (ppm)	RF (W m^{-2})	ΔCO_2 (ppm)	RF (W m^{-2})	ΣC_{seq} (PgC)	ΔCO_2 (ppm)	RF_{final} (W m^{-2})
Enhance land carbon sink							
Afforestation	−41	−0.49	−34	−0.37	183	−16	−0.27
Bio-char production	−10	−0.12	−37	−0.40	399	−34	−0.52
Air capture and storage	−58	−0.69	−186	−1.99	>1000	>|−85|	>|−1.43|
Enhance ocean carbon sink							
Phosphorus addition	−6.5	−0.077	−14	−0.15	574	−52	−0.83
Nitrogen fertilisation	−4.5	−0.054	−9.3	−0.10	299	−25	−0.38
Iron fertilisation	−9.0	−0.11	−19	−0.20	227	−19	−0.29
Enhance upwelling	−0.1	−0.0017	−0.3	−0.0032	16*	−1.9	−0.028
Enhance downwelling	−0.08	−0.00095	−0.18	−0.0019	9*	−1.1	−0.016
Carbonate addition	−0.4	−0.0048	−2.3	−0.025	251*	−30	−0.46

* Activities assumed to continue to year 3000 hence larger airborne fraction than for other ocean options.

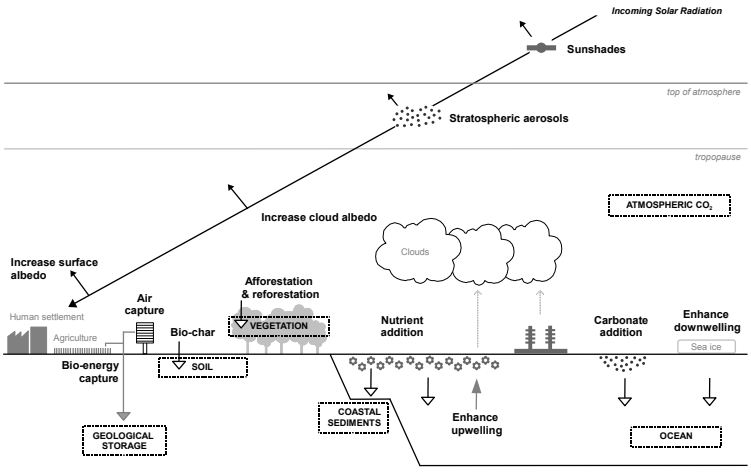

Fig. 1. Schematic overview of the climate geoengineering proposals considered. Black arrowheads indicate shortwave radiation, white arrowheads indicate enhancement of natural flows of carbon, grey downward arrow indicates engineered flow of carbon, grey upward arrow indicates engineered flow of water, dotted vertical arrows illustrate sources of cloud condensation nuclei, and dashed boxes indicate carbon stores. From Vaughan and Lenton (2009), not to scale.